IEEE Access
Multidisciplinary | Rapid Review | Open Access Journal

Received April 23, 2021, accepted May 6, 2021, date of publication May 13, 2021, date of current version May 27, 2021.

Digital Object Identifier 10.1109/ACCESS.2021.3079992

Development and Evaluation of a Smartphone-Based Electroencephalography (EEG) System

ANTHONY D. BATESON[1] **AND AZIZ U. R. ASGHAR**[2]
[1]Department of Engineering, Faculty of Science and Engineering, University of Hull, Hull HU6 7RX, U.K.
[2]Centre for Anatomical and Human Sciences, Hull York Medical School, University of Hull, Hull HU6 7RX, U.K.

Corresponding author: Anthony D. Bateson (a.d.bateson@hull.ac.uk)

This work was supported by the Hull York Medical School Research Committee Funding.

This work involved human subjects or animals in its research. Approval of all ethical and experimental procedures and protocols was granted by the Hull York Medical School Ethics Committee under Application No. 13 03, and performed in line with the WMA Declaration of Helsinki.

ABSTRACT The aim of the study was to design, develop and evaluate a general-purpose EEG platform which integrates with a smartphone. The target specification was a system with 19 EEG channels and data stored onto the smartphone via a Wi-Fi connection. The hardware was developed using three ADS1299 integrated circuits, and the game engine, Unity, was used to develop the smartphone app. An evaluation of the system was conducted using recordings of alpha waves during periods of eye closure in participants (Bland-Altman statistical comparison with a clinical grade EEG system). The smartphone was also used to deliver time-locked auditory stimuli using an oddball paradigm to evaluate the ability of the developed system to acquire event related potentials (ERP) during sitting and walking. No significant differences were found for the alpha wave peak amplitude, frequency and area under the curve for the intra-system (two consecutive periods of alpha waves) or inter-system (developed smartphone-based EEG system versus FDA-approved system) comparisons. ERP results showed the peak amplitude of the auditory P300 component to deviant tones was significantly higher when compared to standard tones for sitting and walking activities. It is envisaged that our general-purpose EEG system will encourage other researchers to design and build their own specific versions rather than being limited by the fixed features of commercial products.

INDEX TERMS Alpha waves, Bland-Altman, EEG, ERP, P300, smartphone.

I. INTRODUCTION

Electroencephalography (EEG) is the measurement of electrical activity from the brain acquired at the scalp surface. It is used to aid the diagnosis of clinical conditions including epilepsy [1], [2], sleep disorders [3] and coma [4] as well as in the study of stroke [5] and brain death [6]. EEG is an established research tool in a wide range of research applications such as brain-computer interfacing (BCI) [7], psychological studies [8], sports activity [9], and emotion monitoring [10].

EEG recordings are traditionally undertaken in restricted laboratory-orientated environments where the system is typically static, of relatively high specification but bulky in weight/size and is directly linked to a PC/laptop [11] for signal capture, processing and analysis. In addition, since EEG signals are in the microvolt range, investigators will typically undertake studies within a controlled environment to minimise noise including electromagnetic interference. Although static EEG systems linked to a PC/laptop in controlled laboratory settings have provided a wealth of scientific output they have limitations. For example, it is difficult to use static EEG systems in natural settings or where participant and device mobilities are required.

The limitations of using static EEG equipment are being addressed by using ambulatory EEG systems. Ambulatory EEG systems have the advantage of being smaller in size/weight and have the capacity to be utilised in a variety of applications and scenarios such as outdoor urban environments [12]–[14], sports performance [15] and brain-computer interfacing [16]–[18]. However, many mobile EEG systems have relatively lower system specifications compared to static EEG systems. For example, in the study by Debener *et al.*

The associate editor coordinating the review of this manuscript and approving it for publication was Mahmoud Al Ahmad.

a wireless EEG headset (14-bit resolution, 128Hz sampling rate, 14 channels) was used to a acquire time-locked auditory event related potentials (ERPs) in combination with a PC mounted within a rucksack on the participant's back during outdoor walking [19]. In investigations using participants walking/running on a treadmill, a higher specification EEG system (24-bit resolution, 512Hz sampling rate, 248 channels) was utilised by mounting all the bulky equipment on an overhead rack [20], [21].

One approach to reducing the weight and size of equipment, improving mobility, and enabling EEG investigations in new settings would be to take a smartphone-based approach. Smartphones are smaller in size and lighter in weight than PCs/laptops and thereby provide a reduction in size/weight that participants are required to carry in EEG investigations. Smartphone technology is improving at a rapid rate [22] with advances in low-power, high-performance microcontroller technology at the centre of these advancements such that the processing capacity differences between smartphones and PCs/laptops is diminishing. Current smartphone devices typically have powerful multi-core processors [23], secure digital (SD) card storage and Wi-Fi connectivity [24] which could all be exploited in the next generation of EEG systems. In addition, the smartphone's range of functionality can be enabled via software application (app) development and apps coded for specific research use cases.

Table 1 lists the published studies which have used EEG systems that link to a smartphone/tablet (in ascending order of publication year). A smartphone-based EEG approach using various operating platforms including iOS and Android have been used in the detection of epileptiform abnormalities [25], [26], BCI for communication [27]–[30], real-time 3D brain imaging of finger movements [31], behind ear monitoring of resting states and auditory evoked potentials [30], [32], [33], driver drowsiness [34], [35], neurofeedback [36] and polysomnography [37]. In published studies that use smartphone-based EEG systems, the range of operations that the smartphone undertakes have included data analysis/classification, stimulus presentation, plotting, relaying data and source reconstruction (Table 1). Whilst all these features are indeed useful in EEG investigations, it would be advantageous to have a smartphone app with the following set of core operations which are required for all EEG recordings: electrode impedance checking, live data plotting and data acquisition/storage.

The studies listed in Table 1 have all used Bluetooth as the wireless technology for communication between the smartphone and the EEG system with the exception of one investigation which used a wired connection [33]. However, Bluetooth has limitations of bandwidth, has relatively slower data rates and is not able to connect to the internet. There is therefore the potential to exploit Wi-Fi technology in smartphone-based EEG systems. Furthermore, by incorporating Wi-Fi communications rather than Bluetooth into the design it allows for future cloud storage and processing of EEG data as well as having potential in clinical and home monitoring applications. Investigators have used a variety of bespoke EEG systems for specific applications, commercial systems (Emotiv EPOC and Smarting) and those which have been modified (Emotiv EPOC) that link to smartphones. Table 1 shows that these systems have a range of sampling rates (128-512Hz) and bit resolutions (8 to 24-bits). The recommendation of the International Federation of Clinical Neurophysiology [38] is for a minimum sampling rate of 200Hz and bit resolution of 12-bit. More than half of the studies listed in Table 1 only have a sampling rate of 128Hz although all investigations have a bit resolution of at least 12-bit. In terms of the number of electrodes used, smartphone-based EEG systems have typically used a limited number (1-16 electrodes). There is a mix of arrangements in the 10/20 configuration and those which are non-standard although two studies have used 24 electrodes in a 10/20 arrangement [30], [39]. Table 1 lists only one smartphone-based EEG study which has used additional differential channels, in this case to acquire electrooculography (EOG) and electromyography (EMG) signals [36]. It would be advantageous to have the ability to acquire such signals in smartphone-based systems as they are useful, for example, for artifact identification and rejection. We applied our previously developed scoring scheme [40] for EEG device mobility (D), participant mobility (P) and system specification (S) to the investigations listed in Table 1. Compared to static EEG systems, the device mobility score for 12 out of 14 smartphone-based EEG studies presented in Table 1 was relatively high at 4D (maximum score = 5), participant mobility in 11 out of 14 studies had low scores of 0-1P (maximum score = 5) and system specification for all studies was relatively low (range 5-12S, maximum score = 20). Recent advances in EEG technologies have enabled systems to be mounted upon the head such as during walking [39] thus providing advantages in terms of reduced electrode displacement and thereby a reduction in artifacts. Scores of device mobility which are $\geq$3 reflect a head-mounted position (Table 1).

Acquiring EEG data from the scalp surface in digital form involves a number of signal processing stages. Integrated circuits (ICs) are now available that can perform these signal processing stages within one component. The ADS1299 (Texas Instruments, USA) is such an IC and makes use of high levels of integration of the various signal processing stages (including gain, analogue to digital conversion and filtering) and has eight differential channels. ADS1299 ICs can be combined to provide a higher number of EEG and differential channels to enable the development of scalable medical instrumentation systems at lower power, smaller size and lower cost [41].

One of the limitations of commercial EEG systems is that it is difficult for researchers to modify the electronics, associated software and features for their specific use cases. The developmental aim of our study was to design a general-purpose EEG platform (smartphone-based EEG system) based upon using ADS1299 ICs which integrate with the

TABLE 1. Smartphone/tablet-based EEG systems utilised in published investigations.

Study	Activity	Smartphone Model: Function	Smartphone link with EEG system	EEG system	Sampling Rate (Hz)	Bit Resolution (bits)	Number of Electrodes	Electrode arrangement	Differential channels	Categorisation of Mobile EEG Scheme (CoME) Score [40]
Campbell [27], 2010	P300-based BCI to choose contact to call	iPhone (iOS, model not stated): partial data analysis, stimulus presentation	Bluetooth	Emotiv EPOC	128	14	16	10/20 arrangement	-	3D, 3P, 6S, 16C
Wang [28], 2011	SSVEP-based BCI	Nokia N97 (Symbian 9.4): data acquisition, plotting and interpretation	Bluetooth	Bespoke	128	12	4	Non-standard, back of the head, around O1/O2	-	4D, 0P, 7S, 4C
Do Valle [25], 2014	Seizure recording with two patients	iPod Touch/iPhone (iOS): data plotting, relaying data to a hospital server	Bluetooth	Bespoke	256	12	1	Behind the ear	-	4D, 3P, 10S, 1C
Stopczynski [31], 2014a	Imagined finger tapping	Galaxy Note, Nexus 7 (Android): data acquisition, analysis and source reconstruction/pre-sentation	Bluetooth	Modified Emotiv EPOC	128	14	14	10/20 arrangement	-	4D, 0P, 6S, 14C
Stopczynski [29], 2014b	BCI-based on imagined finger tapping	Nokia N900 (Maemo 5): data acquisition, analysis and source reconstruction/ presentation	Bluetooth	Modified Emotiv EPOC	128	14	14	10/20 arrangement	-	4D, 0P, 6S, 14C
Wang [34], 2014	Driving simulator	Samsung Galaxy S3 (Android): data analysis, stimulus presentation	Bluetooth	Bespoke	128-512	24	4	Non-standard, occipital region	-	4D, 1P, 7-9S, 4C
Debener [32], 2015	AEP but behind the ear	Sony Xperia Z1 (Android): data acquisition	Bluetooth	Smarting	500	24	8	Behind the ear, c-shape	-	4D, 0P, 12S, 8C
Li [35], 2015	Driver drowsiness detection	Samsung phone (model not stated, Android): partial data acquisition and classification	Bluetooth	Bespoke	128	12	2	10/20 arrangement	-	4D, 1P, 5-7S, 2C
Blum [30], 2017	AEP BCI	Xperia Z1 (Android): data acquisition, recording, stimulus presentation, and online data processing	Bluetooth	Smarting	250	24	24	10/20 arrangement	-	4D, 0P, 11S, 24C
McKenzie [26], 2017	Epileptiform discharge	Nexus 7 (Android): data acquisition	Bluetooth	Modified Emotiv EPOC	128	14	12	10/20 arrangement	-	4D, 0P, 6S, 12C
Wei [36], 2017	Neurofeedback	Phone model not stated: data acquisition, analysis and stimulus presentation	Bluetooth	Bespoke	128	8	1	10/20 arrangement	EOG, EMG	4D, 0P, 9S, 1C
Sterr [37], 2018	Polysomnography	Sony X1 (Windows mobile): data acquisition	Bluetooth	Smarting	250	24	5	Behind the ear, c-shape	-	2D, 1P, 12S, 5C
Salvidegoitia [39], 2019	Episodic memory test while walking outside	Sony Xperia Z1 (Android): data acquisition	Bluetooth	Smarting	500	24	24	10/20 arrangement	-	4D, 3P, 12S, 24C
Sintotskiy [33], 2020	Alpha waves	Phone model not stated: data acquisition	Wired	Bespoke	250	24	2	In-ear	-	4D, 0P, 7S, 2C

capabilities of a smartphone with the capacity for adaptation to a range of specific research uses. Our target system was based upon technical specifications and the 10-20 system configuration for clinical EEG devices [38], and involved developing a system using three combined ADS1299 ICs to form a 24channel system with a resolution of 24-bit and a sampling frequency of 250Hz. The EEG system partners with a smartphone (Android operating system) via a Wi-Fi link with an app developed to have the core features of impedance checking, live data plotting and data acquisition/storage. The mounting position of the EEG system was chosen to be at the waist since the clinically approved device (Morpheus) for comparison is also mounted here. We selected a head cap which was able to link with both the Morpheus and the developed smartphone-based EEG system to enable the convenient EEG system exchange without removal of the head cap. We applied our previously developed scoring scheme [40] for EEG device mobility (D), participant mobility (P), system specification (S) and number of channels (C) to our proposed system which scores as follows: (2D, 3P, 11S, 24C).

For the development of medical devices an evaluation is required against an approved (e.g. US Food Drug Administration, FDA) or established system to determine if they are comparable [42], [43]. Although a statistical correlation approach can be taken to compare two devices, this is questionable for use when attempting to measure agreement between two systems as it measures linear association and not agreement [42], [44]. A commonly accepted and established statistical approach which compares two devices is the Bland and Altman method [42], [44]. This method quantifies the agreement between the measurements from the two devices by plotting the difference on the ordinate axis and the average on the abscissa axis for each measurement pair taken and constructing limits of agreement either side of a mean difference line [45], [46]. In contrast to devices which only acquire a single data measurement and use a Bland and Altman analysis, acquired EEG data comes from a series of samples taken over time and at many scalp electrode locations. It is thus not immediately evident as to which EEG measurement parameter should be selected for the Bland and Altman analysis. One highly identifiable brain oscillation in human participants is the alpha rhythm (8-13Hz) which is recorded in participants with their eyes closed and is dominant in the posterior locations of the head such as at electrode locations O1 and O2 [47], [48]. Power spectral analysis of EEG data during eye closure produces a clear and distinct peak in the alpha frequency range [49]. By extracting features from spectrograms such as the alpha peak power amplitude, peak frequency and area under the curve (AUC) these can be used as the measurements in the Bland and Altman statistical method. This enables comparisons of these alpha wave measurement parameters within the same EEG system (intra-system agreement) and between two EEG systems (inter-system agreement). In the evaluation phase of our study, we compare our developed smartphone-based EEG system to an FDA approved EEG device using a Bland and Altman approach by analysing power spectral features of alpha rhythms in human participants with eyes closed at electrode locations O1 and O2. In addition, we utilise the capability of the smartphone to deliver time-locked auditory stimuli [50] and determine

whether a P300 ERP response could be acquired using the developed smartphone-based EEG system in response to an established oddball paradigm [19], [51]–[53] during sitting. Furthermore, we attempted to make use of the portability of our developed waist-mounted smartphone-based EEG system to determine whether oddball auditory P300 ERPs could be acquired during a walking activity.

II. METHODS

A. ELECTRONIC HARDWARE DEVELOPMENT

Three ADS1299 ICs [41] were interconnected (each channel resolution at 24-bit and 250Hz sampling rate) to achieve an arrangement of 24 differential channels (19 dedicated to EEG). The approach to interconnecting three ADS1299 ICs could have been achieved by using either a daisy-chain mode or standard mode of connection [41]. The standard mode of connection was adopted in the current study, with the three ADS1299 ICs sharing the same serial peripheral interface (SPI) bus connected to a microcontroller, and each ADS1299 IC having an individual chip select pin connection (used for selecting each ADS1299). Connecting the three ADS1299 ICs to a microcontroller in this manner facilitates individual reading/writing of register values and thereby the individual channel configuration which would not have been possible if a daisy-chain mode approach had been taken. The three ADS1299 ICs were synchronised by utilising an external clock signal to maintain synchronous sampling across them.

The process of selecting a microcontroller considered the size and power consumption aspects whilst ensuring that it was also capable of transferring the sampled data via a wireless local area network (LAN) module to a smartphone. An LPC1769 ARM processor [54] was selected as the microcontroller for the design as it provides low power consumption, a small physical footprint and high processing performance relative to its size and power consumption. An RN131 wireless LAN module was connected to the LPC1769 ARM processor via a serial connection (using the RS232 standard) to provide a means of wirelessly connecting to a smartphone via a Wi-Fi link. The Wi-Fi link was further enhanced by using an omni-directional external antenna (Molex, USA) with a gain of 3.5 decibels (dB). The power supply and management of the design was accomplished using a MCP73871 power management IC that allows powering of the system via a lithium-ion battery (3.7V, 2430mAh, Business Batteries, Japan) and charging through a universal serial bus (USB) when connected to a power source. The USB connection was wired to allow firmware updating of the microcontroller to take place via In-Circuit Programming. The functional block diagram of the system developed is shown in Fig. 1. To provide resistance to breakage of the EEG system, all the electronic components of the EEG system were housed in a robust grounded aluminium case with dimensions of 43 $\times$ 78 $\times$ 120mm and 1.5mm in thickness (Hammond Manufacturing, Canada). The overall weight of the developed EEG system was 338g.

B. EMBEDDED SOFTWARE DEVELOPMENT

The embedded software was written in the programming language C [55] because of its common usage and support available in the field of embedded systems. The manufacturer of the LPC1769 microcontroller (NXP, Netherlands) provides a software development environment called LPCXpresso [56], which utilises the C programming language, and was used for the embedded software development. In addition, an operating system (FreeRTOS) was used to provide the software framework and simplify application development and debugging of the EEG system. FreeRTOS is a market leading Real Time Operating System (RTOS) written in the C programming language, and is a free-to-use de-facto standard solution for microcontrollers [57]. FreeRTOS provides support for the chosen microcontroller (LPC1769) along with accompanying software libraries such as support for SPI and RS232 communication protocols. A command line interface facility was available as a part of FreeRTOS, and this was utilised for convenient control of the EEG system. FreeRTOS was used to provide the system with the ability to perform specific tasks under instruction.

C. SMARTPHONE APP DEVELOPMENT

To integrate the Android smartphone with the EEG system, an app was developed using the Unity game engine [58]. The scripts for Unity were developed in the C# language [59]. The main thread of the app utilised a state machine methodology [60] to provide a structured approach towards software development and enabled additional states to be added if required in the future. In the current study, functionality was selected to include impedance checking, live data plotting, ERP (stimulus delivery and acquisition) and data recording via a graphical user interface (GUI). Each feature is enabled by sending a command from the smartphone app to the EEG system. The app subsequently interprets the information returned by the EEG system. In the case of live data plotting, the digital sample values received for each channel were converted into a live plot of the data. When recording EEG data was received over Wi-Fi, the smartphone's free internal storage capacity was utilised by the app. Each EEG data file was stored anonymously under a unique participant number as the filename.

D. EVALUATING THE DEVELOPED SMARTPHONE-BASED EEG SYSTEM: ALPHA WAVES

1) PARTICIPANTS

Twenty-one participants were recruited (range 18 to 55 years, mean $\pm$ standard error of the mean (SEM) age 35.4 $\pm$ 3.1, 5 males and 16 females). Informed written consent was gained from each participant before partaking in the study. The data from one participant was excluded from the analysis due to excessive noise levels in the EEG channels. All participants were healthy with no self-reported history of neurological disorders. The Hull York Medical School Ethics

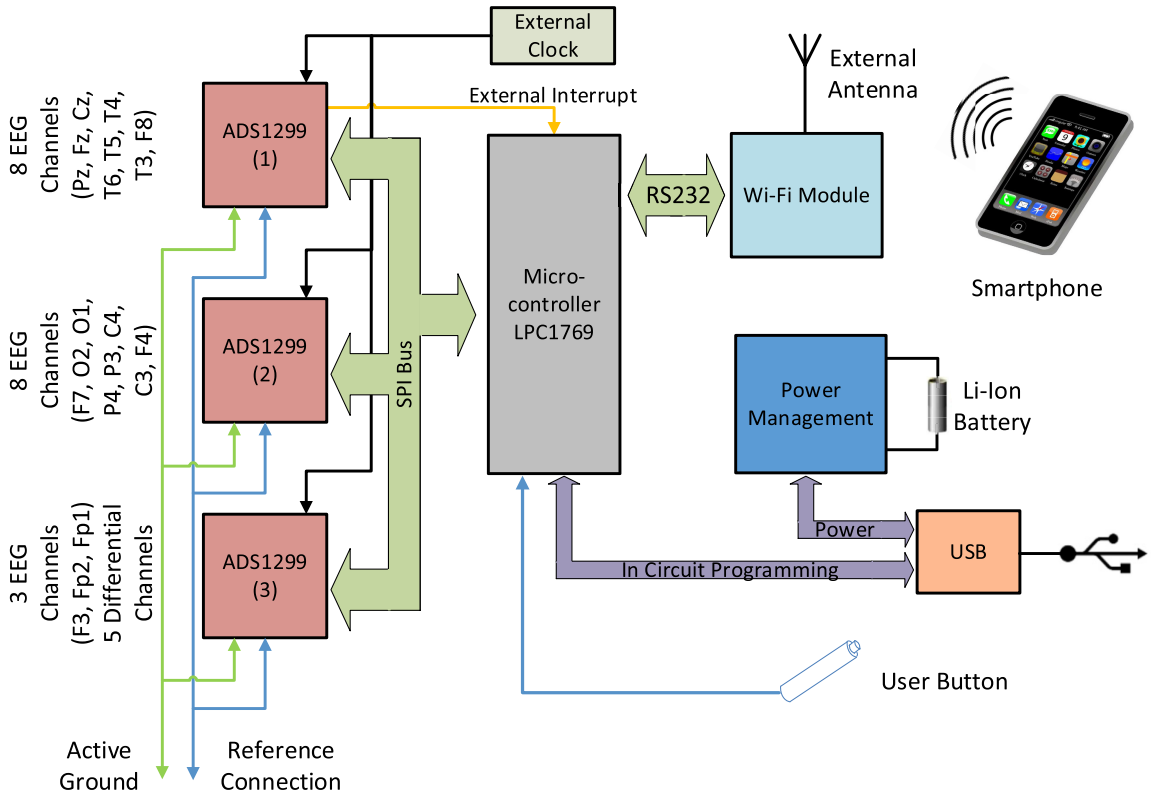

FIGURE 1. The system functional block diagram showing the key sub-systems and their interconnections. The EEG channels, differential channels, active ground and reference connections are labelled. An external interrupt is only taken from the first ADS1299 as all three ADS1299 are synchronised by the external clock. A user button is included for data marking.

Committee provided ethical scrutiny and approval for the study. No monetary compensation was given to participants.

2) EEG SYSTEMS

To enable comparisons to be made with the developed smartphone-based EEG system, a commercial EEG system was used (Morpheus, Micromed, Mogliano Veneto, Italy). The Morpheus system is a clinically FDA approved system with a16-bit resolution and 256Hz sampling rate. The outer dimensions of the Morpheus system are 44 × 83 × 120mm, and a weight of 250g. An EEG head cap with 20 tin electrodes (Softcap, SPES Medica, Italy) was used with 19 electrodes conforming to the international 10/20 standard configuration and a ground electrode connection. The smartphone-based EEG or the Morpheus system was connected to the 19 channel electrode head cap via a 25-way D-type connector. This enabled easy and convenient EEG system exchange with the same head cap without changing the impedance and location of the scalp surface electrodes. When either EEG system was used, they were mounted on the participant via a waist-mounted harness and connected to the same EEG head cap.

3) PARTICIPANT PROTOCOL

The electrode wells of the EEG head cap were filled with conductive gel (Neurgel, SPES Medica, Italy) and the impedance brought below 5kΩ before data acquisition. Each participant continued to wear the same head cap, without removal, while testing each of the EEG systems. All scalp electrodes were referenced to the right ear using an ear clip (EAR1026T0, SPES Medica, Italy). The sequence in which the EEG systems were tested was pseudo-randomised for each participant to mitigate for potential ordering effects of the EEG system used. The testing of the second system was performed within 30 minutes of the first EEG system.

The participants were guided through a protocol of eyes open and eyes closed using recorded audio instructions for each of the two EEG systems under test. To mark the start of eyes open or eyes closed, participants pressed a handheld button connected to the EEG system under test. Each button press generated an event marker on a dedicated channel on the EEG recording. The lying down period (inclined to an angle of 45° whilst supine on a clinical examination couch) was composed of three consecutive periods, each period consisting of 20s of eyes closed followed by 20s of eyes open. The first period of eyes closed/eyes open served to acclimatise the participant to the procedure. The remaining two periods where the eyes were closed are henceforth referred to as period 1 and period 2, respectively, and were used for the intra- and inter-system EEG comparisons. The first 10s of artifact-free data was selected for period 1 and 2 for all participants.

During the protocol using the developed smartphone-based EEG system, the accompanying smartphone (Asus T00G Zenfone 2, Android version 4.3 Jellybean, Quad-core 2.3GHz, 4GB RAM model, free internal storage capacity of 12.2GB) was placed on a bench.

4) ALPHA WAVE ANALYSIS

The data for the Morpheus system (16-bit) and our smartphone-based EEG system (24-bit) were both resampled so that all data was in 16-bit resolution format with a sampling rate of 250Hz. The data was saved in EDF+ file format and imported into the open source software toolbox, EEGLAB [61]. Band pass filtering was performed on the acquired data (0.5 to 40Hz) to filter high frequencies and baseline drift. Artifact free data was identified by visual inspection. Power spectrum density (PSD) plots of the time series data (10s duration) were generated (units: x-axis = Hz, y axis = 10*log10(μV^2/Hz), and the alpha wave peak frequency, amplitude and area under the curve (AUC) determined. The alpha band AUC was defined to be the alpha band power (area under power spectral density 8 to 13Hz) divided by the EEG power in the spectral range 2 to 30Hz based upon the approach of Schier [62]. These three spectral data parameter values (for each individual, for periods 1 and 2) were used to undertake the intra- and inter-system comparisons of the EEG systems.

5) BLAND AND ALTMAN STATISTICAL ANALYSIS

Bland and Altman [44] plots were constructed for the intra- and inter-EEG system comparisons at electrode locations O1 and O2. Since the 95% limits of agreement on a Bland-Altman plot do not comment upon their appropriateness [45], the acceptability level must be defined a priori by the investigator. This is partly based upon making a subjective judgement by considering the context of use, such as clinical importance, and not only upon statistical significance [46]. Bland and Altman have indicated that it is inevitable for at least some lack of agreement between different methods of measurement, but it is to what extent the two systems disagree that is of relevance [46]. We considered and set the following a priori limits of agreement for alpha peak amplitude, AUC and frequency:

a: ALPHA PEAK AMPLITUDE AND AUC

For intra-system comparisons, the alpha peak amplitude/AUC acceptable limits of agreement for the smartphone-based EEG system were set to be equal to or within those obtained for the FDA-approved Morpheus system at each electrode location. For the inter-system comparison, the limits of agreement were set at twice the limits of those for the Morpheus intra-system limits of agreement. Our reasoning here was that, i) although the same head cap was used for both EEG systems, the impedance of electrodes can alter over time leading to a change in waveform peak amplitudes [63]–[65], ii) there is likely to be intra- and inter-participant variations in alpha peak amplitude/AUC over time (EEG data was acquired ∼30 mins apart in the two systems) and iii) there may be variations in the underlying hardware/software for the two EEG systems leading to differences in measurements obtained.

b: ALPHA PEAK FREQUENCY

For intra-system comparisons, the alpha peak frequency limits of agreement were set to be within ±2.5Hz (from the bias line on the Bland-Altman plot). For inter-system comparisons, the limits of agreement were increased by 0.5Hz and set to ±3.0Hz (from the bias line). We selected these a priori values based upon intra- and inter-participant variation that is known to occur for the alpha frequency band oscillation [66], [67], and to account for our EEG data being acquired approximately 30 mins apart for the two EEG systems.

It is appropriate to report confidence intervals (CIs) for bias (mean difference), as well as upper and lower limits of agreement [68]. However, CIs have not been added to the Bland-Altman plots as this detracts from the visual simplicity that is a strength of this technique. Instead, CIs are only reported textually in the Results section. The CIs have been used to ascertain if a bias is significant or not based upon whether the line of equality (zero) is inside or outside the CIs of the bias (mean difference).

E. EVALUATING THE DEVELOPED SMARTPHONE-BASED EEG SYSTEM: AUDITORY P300 ERPs

1) PARTICIPANTS

Paired auditory ERP data (sitting and walking) was acquired from ten participants (age range 18 to 22 years, mean ± SEM age 19.6 ± 0.4, 8 males and 2 females). All participants were healthy with no self-reported history of neurological disorders. The Hull York Medical School Ethics Committee provided ethical scrutiny and approval for the study. No monetary compensation was given to participants.

2) ACQUISITION OF ERPs

We used the same developed smartphone-based EEG system and the head cap as utilised for the alpha waves study. The smartphone was used to deliver the tone stimuli in WAV file format. The incoming ERP data from the EEG system was time marked by the smartphone according to the type of tone presented to the participant (standard or deviant tone). A plug-in for EEGLAB was coded to enable importing of the stored ERP data from the smartphone. This plug-in incorporated an additional 8-bit marker channel required for ERP analysis, with the capacity for up to 255 different events (0 = no marker, 1 to 255 = individual event markers).

3) PARTICIPANT PROTOCOL

Two pure tones were presented binaurally with consumer in-ear headphones (Samsung EO-EG920BW). Both the smartphone and the developed EEG system were housed together in a pouch mounted at the participant's waist. Before the experiment was started, participants were presented with a

brief practice run to establish a comfortable volume and to clarify the distinction between the two tones. Standard (600 Hz) and deviant (1200 Hz) audio tones were presented by the smartphone in a randomized order (ratio of 5 standard to 1 deviant) at a fixed inter-stimulus interval of 1000 ms and a duration of 62 ms. A total of 417 trials were recorded for each participant. Participants were asked to sit (gazed fixed upon a fixation cross), or walk around the perimeter of a $\sim 4 \times 5$m room (usual natural strides with forward gaze), while undergoing the auditory oddball paradigm. The order for sitting and walking was randomised across the participants. Participants were tasked to silently count the number of deviant tones heard.

4) ERP ANALYSIS

For each participant, EEG channels were bandpass filtered from 1 to 30 Hz by implementing a zero-phase Hamming-windowed sinc FIR filter in EEGLAB. Trial epochs for each participant were extracted (−200 to 800 ms) and baseline corrected (−200 to 0 ms). All epochs were included in the analysis for sitting or walking activities. Epochs were averaged to generate standard and deviant ERP waveforms for the sitting and walking activities at Fz, Cz and Pz electrode locations. These fronto-centro-parietal electrode locations were selected as they have previously been shown to generate a clear P300 response [17], [19], [69]. We combined together the ERP waveforms at Fz, Cz and Pz electrodes for the standard tones, and separately for the deviant tones. The peak amplitude of the P300 response for standard and deviant tones was determined as the largest positive peak amplitude between 250 - 500 ms post-stimulus. The associated P300 peak latency was measured as the time to the peak amplitude in the 250-500 ms time window. A paired t-test was used to statistically compare the peak amplitudes between the standard and deviant tones for sitting, and for the walking activity.

III. RESULTS

A. HARDWARE AND SOFTWARE DEVELOPMENT OF THE SMARTPHONE-BASED EEG SYSTEM

Figure 2 shows the smartphone-based EEG system which we developed and named as the ''io:bio'' system. Figure 2a shows the top panel of the system with connections for the EEG channels, the reference electrode and the active ground. The bottom panel has a USB port (for battery charging), a participant event marker push button, various LED indicators and an On/Off switch (Fig. 2b). On the side panel of the system there is a Wi-Fi antenna located under a rubber foam pad (Fig. 2c). The electrical noise floor measured peak-to-peak of the io:bio and Morpheus systems both had an amplitude of approximately 1μV when both sides of a differential channel were shorted.

The smartphone app was coded to provide impedance checking, live data plotting, ERP (stimulus delivery) and data recording via a GUI. Figure 3a shows the main GUI menu that provides access to each of these functions in a simple and intuitive manner. The impedance check feature provides a measure of the impedance of all 19 EEG electrodes via a diagrammatic representation of the electrodes in a 10/20 standard EEG electrode configuration (Fig. 3b). When the impedance of an electrode connection exceeds 8kΩ, the corresponding electrode on the diagram changes to red colour. However, when the impedance of an electrode connection to the scalp is less than 3kΩ, the corresponding electrode on the diagram becomes green in colour. The intermediate range of 3-8kΩ is indicated by the corresponding electrode on the diagram in amber colour. The 'Log Data' feature records the received EEG data onto the smartphone's internal memory storage. Every block of received data is indicated by an incremental count on the smartphone and the time duration of the recording displayed (Fig. 3c). This enables a researcher to detect any loss of data by observing the time count advancing but not the received data count. The live data-plotting feature displays the channels in groups of eight (Fig. 3d).

B. EVALUATING THE DEVELOPED SMARTPHONE-BASED EEG SYSTEM: ALPHA WAVES

Figure 4a,b shows an example of a ten second time series period for each system, taken sequentially in time with the participant lying down with eyes closed at electrode O2. The PSD plots in Fig. 4c show an overlapping profile for channel O2 for both EEG systems. Figure 5 shows comparative bar chart plots (io:bio versus Morpheus) at all 19 EEG channels for the peak amplitude (Fig. 5a), peak frequency (Fig. 5b) and AUC (Fig. 5c) of the alpha waves during eyes closed.

1) BLAND-ALTMAN PLOTS: INTRA-SYSTEM AGREEMENT

Bland-Altman plots were constructed for the alpha peak amplitude intra-system agreement between period 1 versus period 2 of participants lying down with eyes closed using the Morpheus and io:bio systems. Bland-Altman plots for the Morpheus system had limits of agreement ranging from -5.83 to $5.73\mu V^2$/Hz (95% CI -8.22 to -3.44 and 3.34 to 8.12) for channel O1, and -6.73 to $6.14\mu V^2$/Hz (95% CI -9.32 to -4.14 and 3.34 to 8.12) for channel O2 (Fig. 6a). No significant bias towards either period was found for the Morpheus system (O1 bias $= -0.05\mu V^2$/Hz, 95% CI -1.43 to 1.33; O2 bias $= -0.29\mu V^2$/Hz, 95% CI -1.79 to 1.20) as the line of equality resides inside the CIs of each bias. The corresponding Bland-Altman plots for the io:bio intra-system comparison produced limits of agreement ranging from -4.61 to $4.50\mu V^2$/Hz (95% CI -6.49 to -2.72 and 2.62 to 6.39) for channel O1, and -4.27 to $4.46\mu V^2$/Hz (95% CI -9.32 to -4.14 and 3.55 to 8.72) for channel O2 (Fig. 6a). These are within the limits of agreement obtained for the Morpheus system and therefore satisfy the a priori criteria for intra-system agreement. No significant bias towards either period was found for the io:bio system (O1 bias $= -0.05\mu V^2$/Hz, 95% CI -1.14 to 1.04;

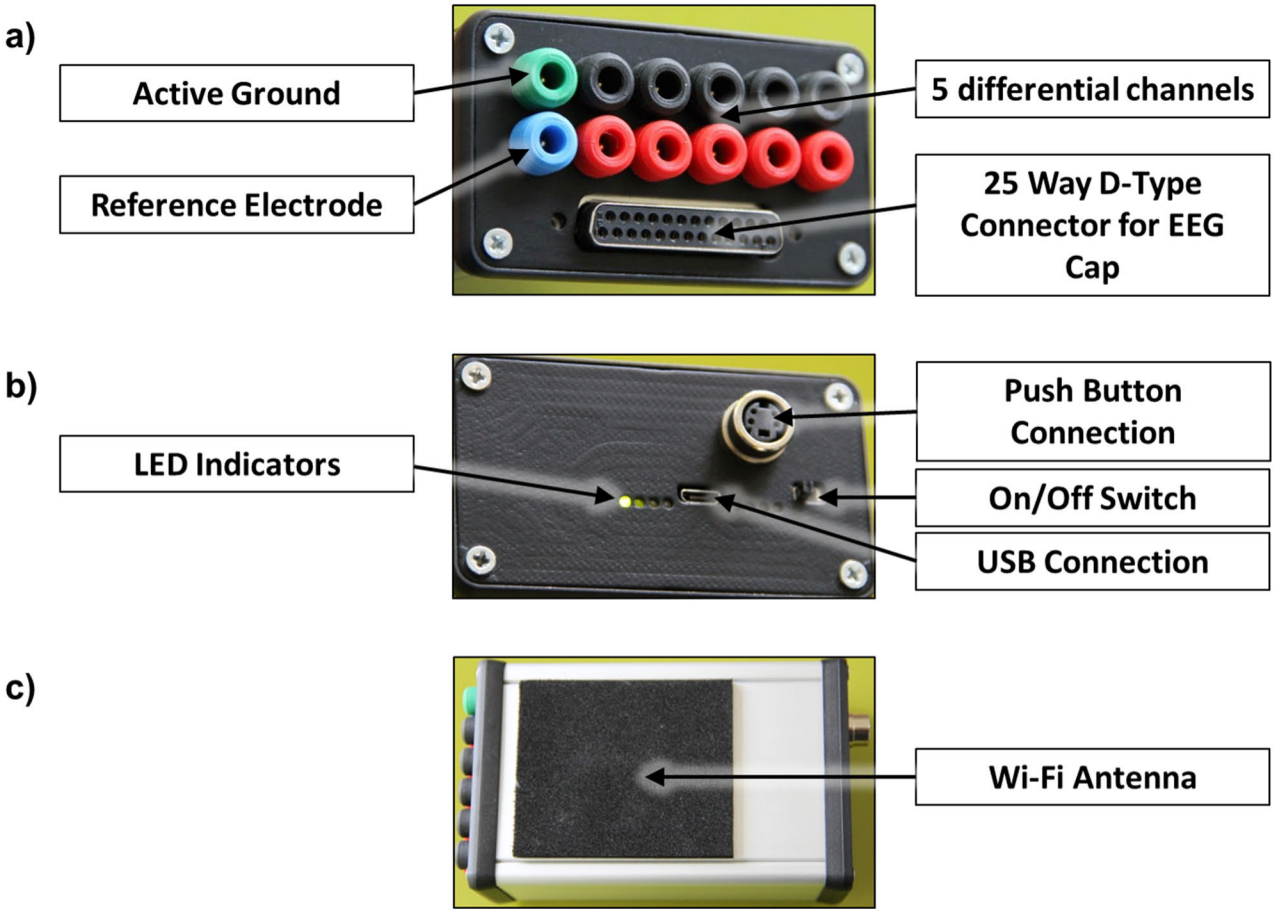

FIGURE 2. Photographs of the developed io:bio smartphone-based EEG system showing a) top panel, b) bottom panel with LED indicators (from left to right: power, charging, connection status and data activity) and c) side panel. The electronics and battery are encased in an aluminium case.

O2 bias = 0.09μV^2/Hz, 95% CI −0.92 to 1.11) as the line of equality resides inside the CIs of each bias.

Bland-Altman plots for the Morpheus system had limits of agreement for the peak frequency ranging from −2.55 to 1.58Hz (95% CI −3.38 to −1.72 and 0.75 to 2.41) for channel O1, and −2.37 to 1.92Hz (95% CI −3.23 to −1.50 and 1.06 to 2.79) for channel O2 (Fig. 6b). No significant bias towards either period was found for the Morpheus system (O1 bias = −0.49Hz, 95% CI −1.43 to 1.33; O2 bias = −0.22Hz, 95% CI −1.43 to 1.33) as the line of equality resides inside the CIs of each bias. The corresponding Bland-Altman plots for the io:bio system produced limits of agreement ranging from −1.60 to 1.84Hz (95% CI −2.29 to −0.91 and 1.15 to 2.53) for channel O1, and −2.73 to 1.76Hz (95% CI −3.64 to −1.83 and 0.85 to 2.66) for channel O2 (Fig. 6b). These are within the limits of agreement obtained for the Morpheus system and therefore satisfy the a priori criteria for intra-system agreement. No significant bias towards either period was found for the io:bio system (O1 bias = 0.12Hz, 95% CI −0.06 to 0.06. O2 bias = −0.49Hz, 95% CI −0.08 to 0.07) as the line of equality resides inside the CIs of each bias.

Bland-Altman plots for the Morpheus system had limits of agreement ranging for the AUC from −0.25 to 0.31 (95% CI −0.36 to −0.13 and 0.19 to 0.43) for channel O1, and −0.26 to 0.30 (95% CI −0.37 to −0.15 and 0.19 to 0.41) for channel O2 (Fig. 6c). No significant bias towards either period was found for the Morpheus system (O1 bias = 0.03, 95% CI −0.04 to 0.10; O2 bias = 0.02, 95% CI −0.04 to 0.09) as the line of equality resides inside the CIs of each bias. The corresponding Bland-Altman plots for the io:bio system produced limits of agreement ranging from −0.26 to 0.26 (95% CI −0.36 to −0.15 and 0.15 to 0.36) for channel O1, and −0.33 to 0.32 (95% CI −0.36 to −0.15 and 0.15 to 0.36) for channel O2 (Fig. 6c). These are within the limits of agreement obtained for the Morpheus system and therefore satisfy the a priori criteria for intra-system agreement. No significant bias towards either period was found for the io:bio system (O1 bias = 0.00, 95% CI −0.06 to 0.06; O2 bias = −0.01., 95% CI −0.08 to 0.07) as the line of equality resides inside the CIs of each bias.

2) BLAND-ALTMAN PLOTS: INTER-SYSTEM AGREEMENT

Bland-Altman plots were constructed for inter-system agreement between Morpheus versus io:bio systems for peak amplitude. Bland-Altman plots comparing the two systems for agreement for period 1 has limits of agreement

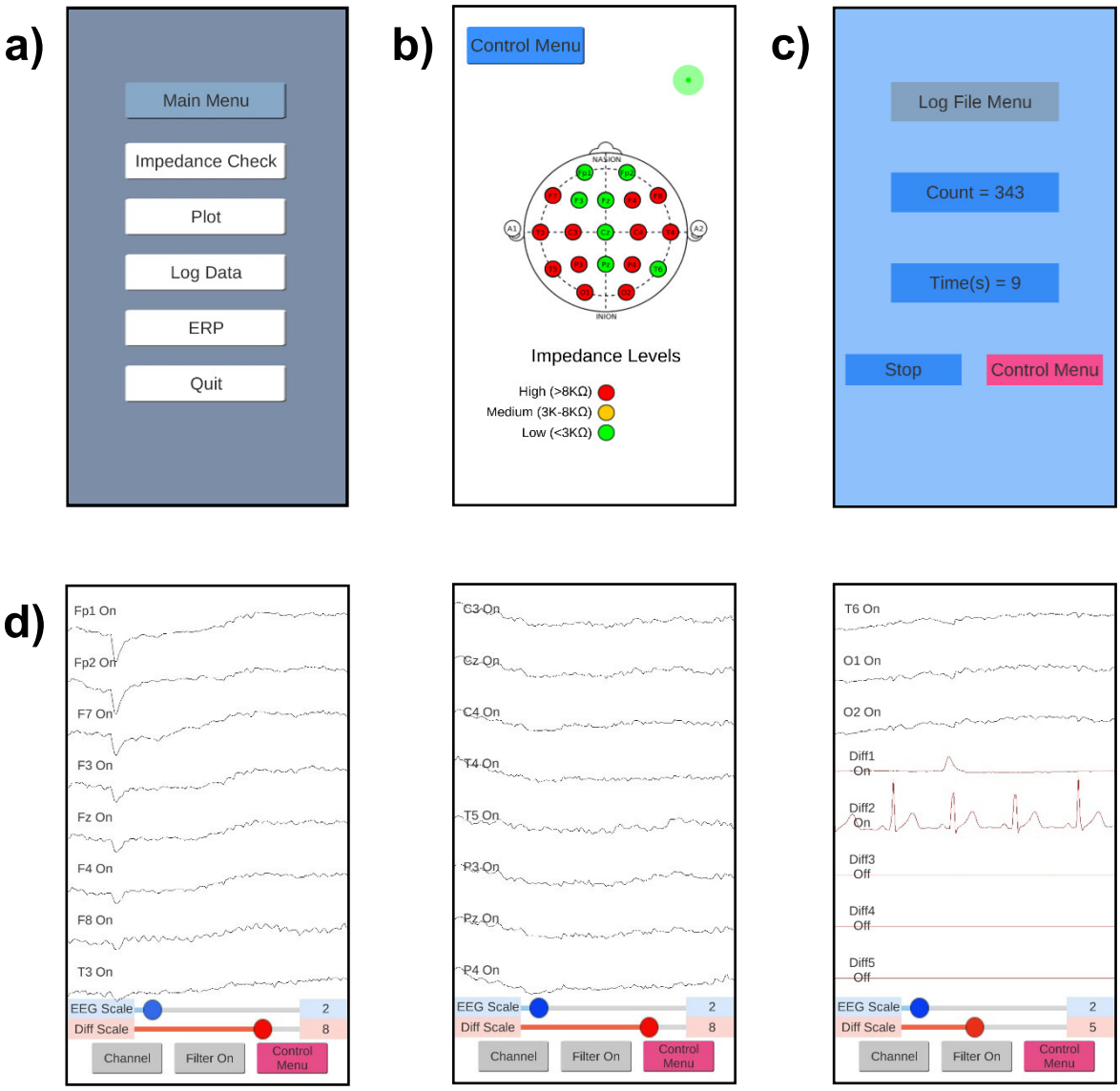

FIGURE 3. Smartphone app showing a) main GUI menu, b) impedance checking, c) data recording and d) live data plotting (high pass filtering 0.1Hz) of 19 EEG channels, an EOG channel (Diff 1) and an ECG channel (Diff 2). Note that a blink artifact is visible in the frontal EEG electrodes.

ranging from −11.54 to 8.21μV^2/Hz (95% CI −15.62 to −7.46 and 4.12 to 12.29) for channel O1, and −11.51 to 7.61μV^2/Hz (95% CI −15.36 to −7.66 and 3.77 to 11.46) for channel O2 (Fig. 7a). The limits of agreement for period 2 range from −12.56 to 9.21μV^2/Hz (95% CI −17.06 to −8.05 and 4.71 to 13.71) for channel O1, and range from −12.85 to 9.74μV^2/Hz (95% CI −17.39 to −8.31 and 5.20 to 14.29) for channel O2 (Fig. 7a). No significant bias towards either system was found for period 1 (channel O1 bias = −1.67μV^2/Hz, 95% CI −4.03 to 0.69; O2 bias = −1.95μV^2/Hz, 95% CI −4.17 to 0.27) or for period 2 (O1 bias = −1.67μV^2/Hz, 95% CI −4.27 to 0.93; O2 bias = −1.55μV^2/Hz, 95% CI −4.18 to 1.07) as the line of equality resides inside the CIs of each bias.

Bland-Altman plots comparing the two systems for agreement for periods 1 have peak frequency limits of agreement ranging from −3.32 to 2.10Hz (95% CI −4.42 to −2.23 and 1.01 to 3.19) for channel O1, and −1.91 to 1.93Hz (95% CI −2.67 to −1.13 and 1.16 to 2.70) for channel O2 (Fig. 7b). The limits of agreement for period 2 range from −1.93 to 1.93Hz (95% CI −2.71 to −1.16 and 1.16 to 2.71) for channel O1 and from −2.54 to 2.03Hz (95% CI −3.45 to −1.62 and 1.11 to 2.94) for channel O2 (Fig. 7b). No significant bias towards either system was found for period 1 (channel O1 bias = −0.61Hz, 95% CI −1.24 to 0.02; O2 bias = 0.01Hz, 95% CI −0.43 to 0.46) or for period 2 (O1 bias = 0Hz, 95% CI −0.45 to 0.45; O2 bias = −0.26Hz, 95% CI −0.79 to 0.27) as the line of equality resides inside the CIs of each bias.

For AUC, Bland-Altman plots comparing the two systems using period 1 have limits of agreement ranging from −0.38 to 0.41 (95% CI −0.54 to −0.22 and 0.24 to 0.57) for channel O1, and −0.35 to 0.40 (95% CI −0.50 to −0.20 and

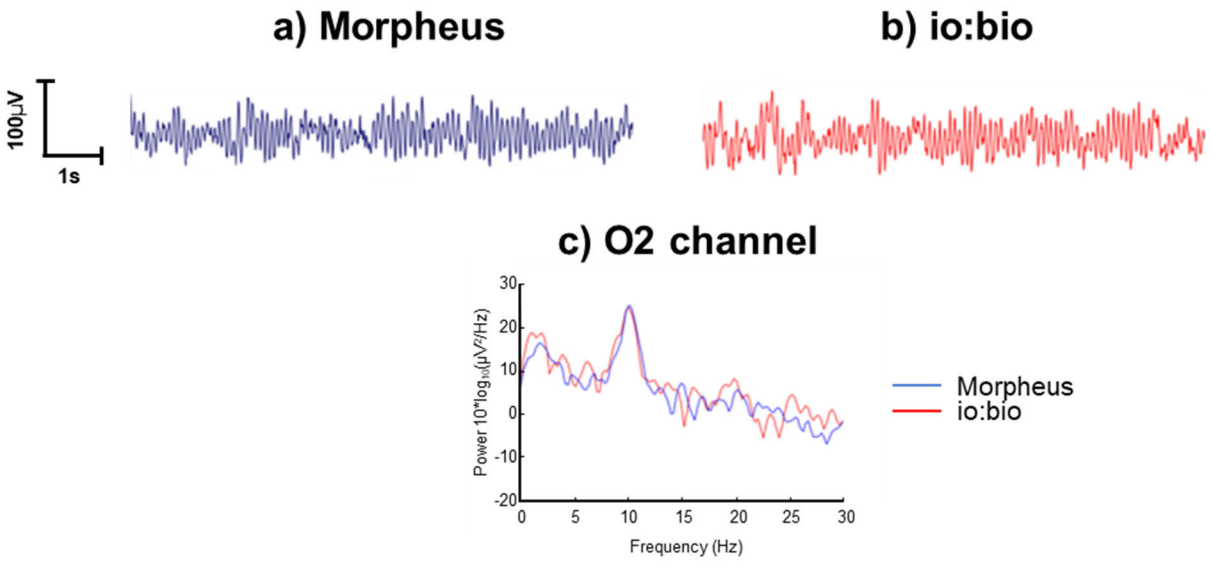

FIGURE 4. Example 10s periods of a single participant's time series EEG trace taken sequentially during period 1 of lying down with eyes closed for the a) Morpheus and b) io:bio systems at channel location O2 and c) the respective PSD plots for the two systems at electrode O2.

0.25 to 0.55) for channel O2 (Fig. 7c). The limits of agreement for Period 2 range from −0.48 to 0.45 (95% CI −0.67 to −0.29 and 0.26 to 0.64) for channel O1 and from −0.46 to 0.46 (95% CI −0.65 to −0.28 and 0.28 to 0.65) for channel O2 (Fig. 7c). No significant bias towards either system was found for period 1 (channel O1 bias = 0.01, 95% CI −0.08 to 0.11; O2 bias = 0.03, 95% CI −0.06 to 0.12) or for period 2 (O1 bias = −0.02, 95% CI −0.13 to 0.10; O2 bias = 0, 95% CI −0.11 to 0.11) as the line of equality resides inside the CIs of each bias.

C. EVALUATING THE DEVELOPED SMARTPHONE-BASED EEG SYSTEM: AUDITORY P300 ERPs

The deviant tones, delivered by the smartphone to participants via headphones, evoked P300 ERP waveforms for sitting, and for the walking activity. Figure 8 shows the ERP plots for the grand mean P300 responses to standard and deviant tones during sitting and walking for combined Fz + Cz + Pz electrodes. A visual inspection of the pre-tone stimulus period indicates a higher level of baseline noise for walking compared to sitting (Fig. 8a,b). A statistically significant higher peak amplitude was found for the P300 deviant tone compared to the standard tone for sitting or walking (Table 2). There were no significant difference for the P300 peak latency between the deviant and standard tones for sitting or for the walking activity ($p > 0.05$, paired t-test).

IV. DISCUSSION

In this study we have designed and developed a general-purpose smartphone-based EEG platform which we have named ''io:bio''. The io:bio smartphone-based EEG system and associated app was evaluated against a clinical grade FDA approved system in human participants using recordings of alpha waves during periods of eye closure. No significant differences were found for the intra-system or inter-system comparisons using a Bland-Altman statistical approach. Furthermore, we were able to acquire using the developed smartphone-based EEG system P300 ERPs in response to an auditory oddball paradigm during sitting and walking activities. Our developed smartphone-based EEG system has therefore the potential to be utilised in a plethora of applications and environments.

The hardware design architecture consisted of three ADS1299 ICs. Their connection to the microcontroller was achieved using a standard mode of connection rather than a daisy-chain connection. This mode of connection enabled configuration of the gain settings for each channel independently as indicated in the ICs datasheet [41]. Had this connection approach not been taken, the ability to use channels for other applications such as EMG, ECG or EOG, which have larger signal amplitudes, would not have been possible as all channels would have had the same settings for gain which could result in signal clipping. The design approach taken relies upon the microcontroller having sufficient time to read the data from each ADS1299 IC in turn before the next hardware interrupt, and in turn new data is received. Increasing sampling rates will reduce the time period available to achieve the necessary data transfer and this will necessitate a higher performance microcontroller to support the higher sampling rates available via the ADS1299 IC. The Wi-Fi module is communicated to via a serial connection; this is a performance limitation of the current design as the maximum data rate of the system cannot exceed this limit. A Wi-Fi module with an SPI interface and higher bandwidth could be used to support higher sampling rates but would come at the cost of higher power consumption. The higher power consumption could be mitigated by using a battery with an

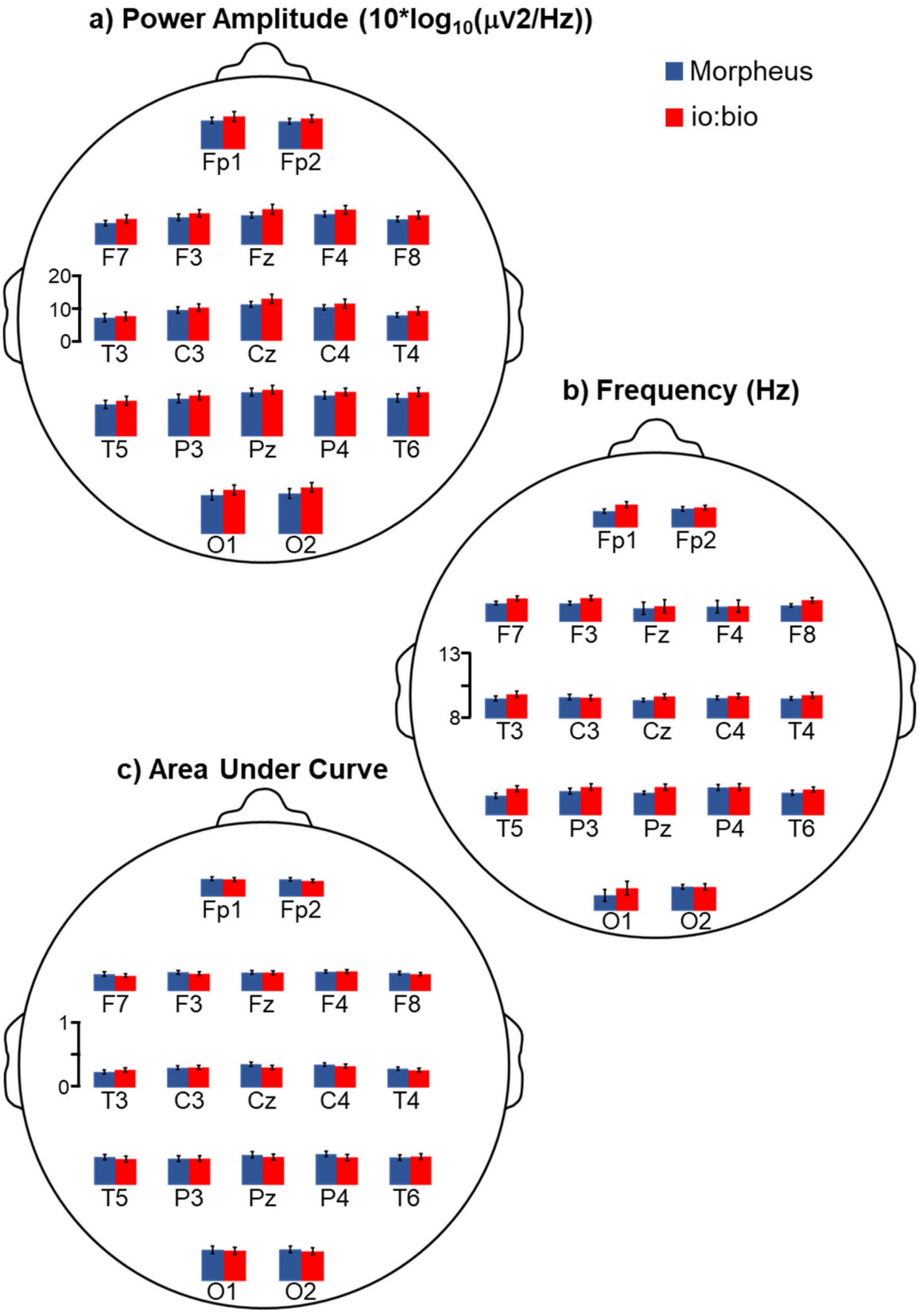

FIGURE 5. Comparison of Morpheus and io:bio systems during period 2 of eyes closed for alpha band a) peak power amplitude, b) peak frequency, and c) area under the curve (normalised). Data are presented as mean ± SEM (n = 16-21).

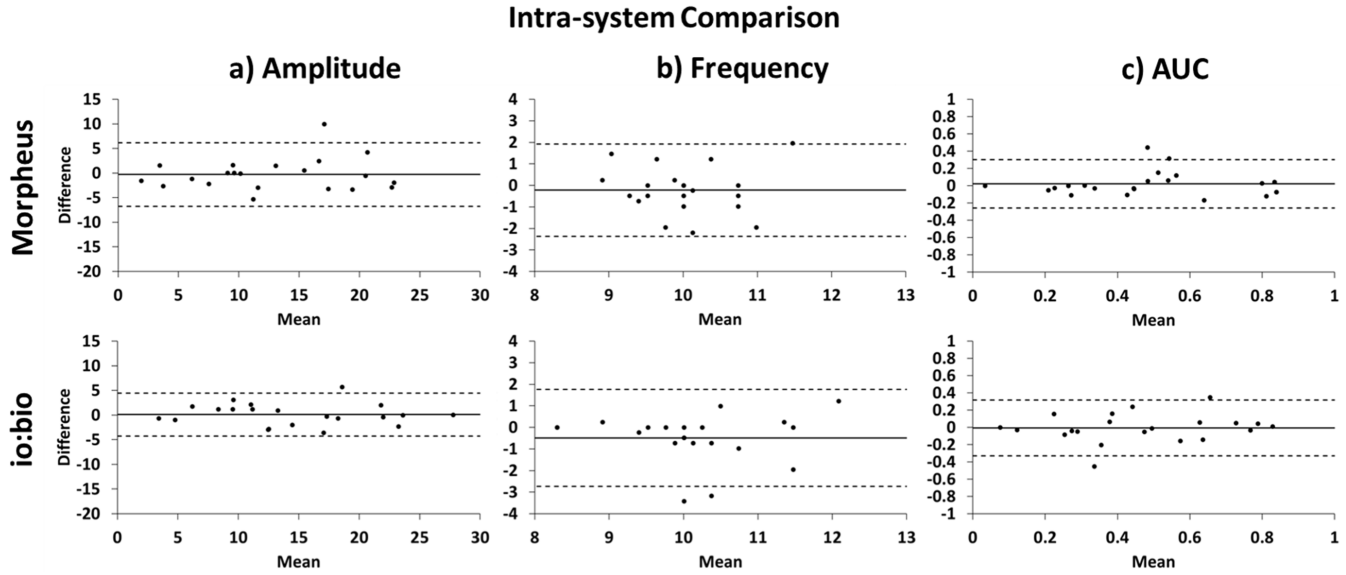

FIGURE 6. Bland-Altman plots for alpha peak a) amplitude, b) frequency and c) AUC intra-system comparisons made using Morpheus or io:bio systems during participants lying down with eyes closed at electrode O2 (n = 20). The x-axis represents the mean [(period 1 + period 2)/2] and the y-axis the difference (period 1 – period 2) for each pair of measures, for the Morpheus and io:bio systems.

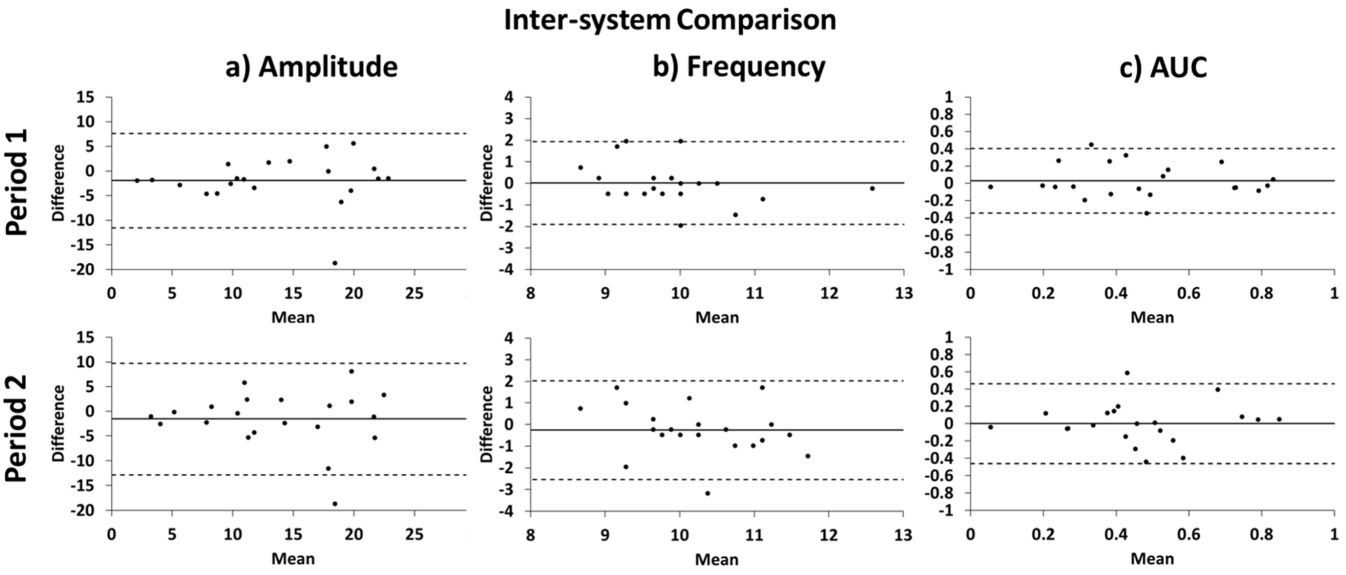

FIGURE 7. Bland-Altman plots for alpha peak a) amplitude, b) frequency and c) AUC inter-system comparisons made between the Morpheus and io:bio systems during participants lying down with eyes closed at electrode O2 (n = 20). The x-axis represents the mean [(Morpheus + io:bio)/2)] and the y-axis the difference (Morpheus - io:bio) for each pair of measures, for periods 1 and 2.

increased storage capacity but this would increase the overall system size and weight.

A. DEVELOPMENT OF THE SMARTPHONE-BASED EEG SYSTEM

Our io:bio smartphone-based EEG system specification used three ADS1299 ICs in standard configuration to enable the recording of EEG channels with a sampling frequency of 250Hz at a resolution of 24-bit. This specification exceeds the recommendation of the International Federation of Clinical Neurophysiology [38] of a minimum sampling rate of 200Hz and bit resolution of 12-bit. As the ADS1299 IC has the capability for data sampling rates of up to 16kHz, it is possible to have system specifications where higher sampling rates are required. For example, higher rates are required by epileptologists to record ultra-fast oscillations [70] and for perceptual and cognitive processing investigations related to autism [71]. However, with higher sampling rates there will be increased demands upon the systems microcontroller along with the requirements for a higher bandwidth from the Wi-Fi module and additional data storage capacity. Our io:bio system was developed at 24-bit resolution,

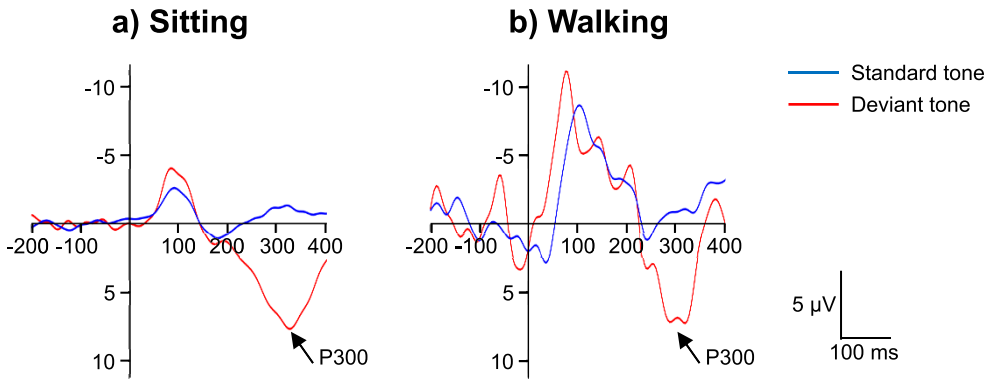

FIGURE 8. Grand mean P300 waveforms for standard and deviant tones during participant a) sitting and b) walking for combined Fz + Cz + Pz electrodes using the developed waist-mounted io:bio smartphone-based ERP system (n = 10).

TABLE 2. Grand mean peak amplitude and latency for the P300 ERP component in response to standard and deviant tones during participant sitting and walking for combined Fz + Cz + Pz electrode locations using the developed io:bio smartphone-based ERP system (n = 10).

	Standard Tone		Deviant Tone	
Activity	**Peak Amplitude (μV)**	**Peak Latency (ms)**	**Peak Amplitude (μV)**	**Peak Latency (ms)**
Sitting	1.4 ± 1.6	389 ± 24	10.7 ± 2.1*	329 ± 11
Walking	2.7 ± 1.5	372 ± 28	13.2 ± 2.4*	352 ± 22

*Statistically significant greater peak amplitude for the deviant tone compare to the standard tone ($p < 0.05$, paired t-test).

which is the same resolution as some of the studies listed in Table 1 [30], [32]–[34], [37], [39], and is at the upper level of resolution for smartphone-based EEG systems.

We opted in our io:bio smartphone-based EEG system to utilise Wi-Fi technology, instead of Bluetooth, for the wireless link between the acquisition electronics and the smartphone. In contrast, all the smartphone/tablet-based EEG investigations listed in Table 1 have used Bluetooth technology. Although Bluetooth allows peer-to-peer connection, it has limitations in its communication range available compared to Wi-Fi and has no capability to connect to network infrastructure. For example, in the smartphone-based EEG study by Blum *et al.* [30], the Bluetooth used has a restricted range (SMARTING system, range of 10 metres). Bluetooth also has limitations in data rate, which are generally lower than Wi-Fi, and is less energy efficient [72]. Unlike Bluetooth, Wi-Fi can be used for both peer-to-peer connection and connection to a network infrastructure such as a hospital, home or research facility. Such Wi-Fi enabled network connection allows for functions such as data cloud storage/processing and is therefore advantageous in terms of future research potentials related to clinical and home monitoring applications. Furthermore, by using Wi-Fi rather than Bluetooth it is possible to dispense with the participant having to carry the smartphone in locations where Wi-Fi coverage is available.

Our developed io:bio EEG system was similar in size dimensions and weight to the Morpheus system. To enable greater resistance to possible breakage, we encased our developed io:bio system in a robust aluminium case instead of a plastic encasement. A robust encasement would be desirable if EEG studies were required to be undertaken in real-world environments outside the laboratory setting such as urban environments [12], [73], [74], whilst walking [20], [75]–[77] and rehabilitation applications [78], [79]. The underlying design of our io:bio system could be adapted for utility in consumer-orientated EEG applications, as was undertaken in the investigations by Khushaba *et al.* [80] and Yadava *et al.* [81] using a plastic head-mounted case. In addition, it should be feasible to integrate our EEG electronics into

wearable fabrics such as a head cap or helmet using a flexible PCB approach [32], [82], [83].

As is possible with the FDA-approved Morpheus system, the io:bio system was also able to acquire data from 19 EEG channels (in standard 10-20 configuration). Previous investigations using smartphone-based EEG systems have recorded from a relatively low number of EEG channels (ranging from 1-16 channels) in either 10-20 arrangements or in non-standard configurations (see Table 1). The 10-20 electrode arrangement offers the advantages of convenient and expeditious participant set up times and enables standardised testing to allow comparisons with the results of the EEG literature. There is the potential to increase the number of EEG channels in our developed io:bio system. For instance, a smartphone-based EEG system could be developed which has the capability to record using the 10-10 or 10-5 electrode arrangements [84]. This could be achieved by incorporating additional ADS1299 ICs to our existing electronics architecture. However, a more powerful microprocessor and a Wi-Fi module with higher bandwidth are likely to be required to process the additional data throughput.

Our developed EEG io:bio system was paired via Wi-Fi to a smartphone running the Android operating system. Compared with tethering the EEG system to a PC/laptop, our smartphone-based approach has advantages in terms of size, weight and thereby greater portability of the system. Such portability of the smartphone could be exploited in research investigations which aim to acquire EEG data in natural/real-life settings such as outdoor urban environments [12], [13] or sports activities [15]. Furthermore, a smartphone-linked EEG system offers the experimenter the potential for higher levels of participant mobility as there is no physical tethering to a PC/laptop (see Bateson *et al.* [40]). In our study, we used a relatively inexpensive smartphone and were able to successfully acquire and store data from all 24 differential channels along with a marker channel. The free internal storage capacity of 12.2GB in the smartphone used in our current study is likely to be of sufficient memory capacity for the majority of EEG investigations including those where 24 hour recordings are required [85] as the system will generate approximately 64Mb of data per hour. However, if higher sampling rates and number of channels are required this would lead to larger file sizes. In this scenario an SD card could be installed or a smartphone utilised which has a higher capacity internal memory.

In our current study, the functions of the smartphone focused upon checking impedance at each EEG electrode, plotting live data, and acquisition/storage of data via a GUI as we regarded these as core features required in any EEG investigation. We envisage that minimising the app to these core functions in the current configuration would enable more intuitive operation of the smartphone-based EEG system by the non-specialist. The core functions we developed were achieved by coding an app for the smartphone using the game engine, Unity. A major benefit of using Unity is that it opens the potential for future deployment of our app to additional platforms such as iOS, PC/laptop, virtual reality or augmented reality headsets, games consoles and smart TVs. Such deployment to these platforms in conjunction with the io:bio EEG system could be used to advance neurofeedback systems [29], [78], [86], gamification projects [87]–[89] and BCI testbeds [90], [91]. There is opportunity for future expansion of the features on our smartphone app by utilising Unity. For instance, additional functionality could be added to our app, as has been incorporated by other investigators in their smartphone-based EEG systems, for stimulus presentation [27], [34], [36], data interpretation [28], [34], source reconstruction [29], classifiers [35], and relaying data to external servers [25]. However, these applications are likely to require a smartphone with higher specification and performance capabilities than the one used in the current study.

B. EVALUATION OF THE SMARTPHONE-BASED EEG SYSTEM: ALPHA WAVES

To test intra-system repeatability we determined the alpha wave peak amplitude, frequency and AUC from PSD plots in both the Morpheus EEG system versus the io:bio smartphone-based system at occipital electrode locations. For the FDA-approved Morpheus system, the Bland and Altman plots showed no significant bias between the two consecutive alpha activity test periods thus showing intra-system repeatability. The Bland-Altman plots for the io:bio system had limits of agreement which were within the limits of agreement obtained for the Morpheus system and therefore satisfied our a priori criteria for intra-system agreement. As found for the Morpheus system, there was no significant bias towards either test period demonstrating the intra-system repeatability when using the io:bio smartphone-based system. The intra-system repeatability [45] is a critical feature when utilising EEG systems within clinical and research settings, and since the io:bio system has comparable system repeatability to the FDA-approved Morpheus system it should have utility in these environments.

The results obtained in the current study for inter-system variability (Morpheus versus io:bio systems) were within our a priori limits of agreement. The Bland and Altman plots indicate that the io:bio smartphone-based EEG system can therefore be used interchangeably with the Morpheus system. The limits of agreement in the Bland-Altman plots for inter-system variability were wider for peak amplitude and AUC compared to the intra-system plots for Morpheus or the io:bio smartphone-based system. These wider inter-system limits could be accounted for by potential differences in measures obtained when testing and comparing any two electronic systems. In addition, the wider limits could be attributed to the greater time period lapsed between testing the two EEG systems in a sequential order. One limitation of the Bland and Altman approach is that a subjective judgement is required to be made by the investigator of what constitutes an acceptable limit of agreement [42]. This is made more challenging as the spectral EEG for inter-individual variation is higher compared to the intra-individual variation [92].

In the current investigation, we used a sequential methodological recording approach for the comparisons between two EEG systems. An alternative approach is to record simultaneously from two EEG systems. For instance, in the study by Badcock *et al.* [93] two separate electrode arrangements were configured onto the head to compare the EPOC Emotiv system with the Neuroscan Synamps one. This involved cutting slits in the electrode head cap for the Neuroscan Synamps to allow electrodes of the EPOC Emotiv to be inserted onto the scalp surface. We did not take this approach as electrodes would not have been in the exact same location between the two EEG systems making it difficult to interpret the data and evaluate the test EEG system. Jackson *et al.* [94] and Omurtag *et al.* [95] used an approach where both EEG systems were connected to a single electrode head cap in parallel using a signal splitter arrangement. This has the advantage of being able to record simultaneously from the same electrode sites. However, it is possible that potential system interactions could occur while the two systems are connected simultaneously, and we therefore did not adopt this approach. Perhaps a future approach could be to combine our approach with that of Jackson *et al.* [94] and Omurtag *et al.* [95] to determine how the two systems would perform under the same experimental conditions when connected separately and simultaneously.

C. EVALUATION OF THE SMARTPHONE-BASED EEG SYSTEM: AUDITORY P300 ERP

We utilised the processing capabilities of a smartphone to deliver time-locked auditory stimuli to participants via headphones, and captured the ERP data using the developed io:bio EEG system. Using this novel smartphone-based ERP acquisition arrangement, we found significantly higher peak amplitudes of the P300 component to the deviant tone condition compared to the standard tone for the sitting activity. This result is in line with previous studies which have demonstrated that the P300 response to a deviant/uncommon tone is greater in amplitude compared to a standard/common tone [19], [96]. Using the developed waist-mounted smartphone-based io:bio system we sought to determine if P300 auditory oddball ERP's could be acquired in participants undertaking a walking activity. We observed a clear P300 ERP response to deviant tones. As for sitting, the P300 ERP was significantly greater in peak amplitude to the deviant tone condition compared to the standard tone. Similar amplitude auditory oddball P300 ERP responses to deviant tones have been reported during walking although the baseline noise was less compared to our results as a head-mounted EEG system was used [19].

D. FUTURE DIRECTIONS

In our current study we compared the developed io:bio system with the Morpheus system in terms of the noise floor and alpha waves during eyes closed using a Bland and Altman statistical approach. There are many other additional comparisons which could be undertaken in future comparative evaluation studies of a developed EEG system with a clinically approved or commercial EEG system which present, for example, visual, auditory or somatosensory stimuli or those which present cognitive paradigms. Although commercial smartphone-based EEG systems are becoming available, an advantage of developing bespoke smartphone-based EEG systems such as the io:bio is that specific modifications/enhancements can be readily made. Additional hardware or existing features of the smartphone could be incorporated into our smartphone-based EEG system. Some examples include 3D accelerometery, motion sensing and GPS for determination of geographical location/participant tracking by the smartphone. A head-mounted configuration of our io:bio system could also be developed based upon the EEG system functional block diagram in Fig. 1. This advancement would have the advantage of enabling greater mobility of participants, reduced noise from EEG electrode displacements thereby enabling the acquisition of EEG/ERP data in natural/real-life environments. Our ERP study could be extended to time-locked visual stimuli delivered to participants via the smartphone's screen. Whilst all of the proposed developments are potentially achievable, each development would require its own separate evaluation.

V. CONCLUSION

We have developed and evaluated a general-purpose smartphone-based EEG platform utilising a novel Wi-Fi communications approach. The system and associated smartphone app is able to record data onto a smartphone's internal memory via a Wi-Fi link. The smartphone-based EEG system was evaluated against an FDA-approved EEG system in human participants. Using recordings of alpha waves, no significant differences were found in the results for intra-system or inter-system comparisons using a Bland-Altman plot analysis approach suggesting that the two systems can be used interchangeably. In addition, we utilised the capability of the smartphone to deliver time-locked auditory stimuli and acquired P300 ERPs in response to an oddball paradigm during sitting and walking activities. Our smartphone-based EEG system has the potential to be modified, unlike commercial systems, for specific researcher-envisaged use cases.

ACKNOWLEDGMENT

The authors are grateful to Peter Lobo-Kazinczi for his technical assistance in the design and population of the circuit board of the EEG system, and to Murat Aksoy for assistance in the ERP data analysis.

REFERENCES

[1] D. Velis, P. Plouin, J. Gotman, and F. L. da Silva, "Recommendations regarding the requirements and applications for long-term recordings in epilepsy," *Epilepsia*, vol. 48, no. 2, pp. 379–384, Feb. 2007, doi: 10.1111/j.1528-1167.2007.00920.x.

[2] U. Seneviratne, A. Mohamed, M. Cook, and W. D'Souza, "The utility of ambulatory electroencephalography in routine clinical practice: A critical review," *Epilepsy Res.*, vol. 105, pp. 1–12, Jul. 2013. [Online]. Available: http://www.sciencedirect.com/science/article/pii/S0920121113000429

[3] D. Liu, Z. Pang, and S. R. Lloyd, "A neural network method for detection of obstructive sleep apnea and narcolepsy based on pupil size and EEG," *IEEE Trans. Neural Netw.*, vol. 19, no. 2, pp. 308–318, Feb. 2008.

[4] J.-M. Guärit, D. Verougstraete, M. de Tourtchaninoff, D. Debatisse, and C. Witdoeckt, "ERPs obtained with the auditory oddball paradigm in coma and altered states of consciousness: Clinical relationships, prognostic value, and origin of components," *Clin. Neurophysiol.*, vol. 110, no. 7, pp. 1260–1269, Jul. 1999, doi: 10.1016/S1388-2457(99)00061-9.

[5] J. L. De Reuck, "Stroke-related seizures and epilepsy," *Neurologia Neurochirurgia Polska*, vol. 41, no. 2, pp. 144–149, 2007.

[6] J. Cao and Z. Chen, "Advanced EEG signal processing in brain death diagnosis," in *Signal Processing Techniques for Knowledge Extraction and Information Fusion*. Boston, MA, USA: Springer, 2008, pp. 275–298.

[7] M. De Vos, M. Kroesen, R. Emkes, and S. Debener, "P300 speller BCI with a mobile EEG system: Comparison to a traditional amplifier," *J. Neural Eng.*, vol. 11, no. 3, Jun. 2014, Art. no. 036008, doi: 10.1088/1741-2560/11/3/036008.

[8] R. Thibodeau, R. S. Jorgensen, and S. Kim, "Depression, anxiety, and resting frontal EEG asymmetry: A meta-analytic review," *J. Abnormal Psychol.*, vol. 115, no. 4, p. 715, 2006.

[9] T. Thompson, T. Steffert, T. Ros, J. Leach, and J. Gruzelier, "EEG applications for sport and performance," *Methods*, vol. 45, no. 4, pp. 279–288, Aug. 2008.

[10] M. Murugappan, R. Nagarajan, and S. Yaacob, "Combining spatial filtering and wavelet transform for classifying human emotions using eeg signals," *J. Med. Biol. Eng.*, vol. 31, no. 1, pp. 45–51, 2011.

[11] J. T. Gwin, K. Gramann, S. Makeig, and D. P. Ferris, "Removal of movement artifact from high-density EEG recorded during walking and running," *J. Neurophysiol.*, vol. 103, no. 6, pp. 3526–3534, Jun. 2010, doi: 10.1152/jn.00105.2010.

[12] P. Aspinall, P. Mavros, R. Coyne, and J. Roe, "The urban brain: Analysing outdoor physical activity with mobile EEG," *Brit. J. Sports Med.*, vol. 49, no. 4, pp. 272–276, Feb. 2015, doi: 10.1136/bjsports-2012-091877.

[13] E. Wascher, H. Heppner, and S. Hoffmann, "Towards the measurement of event-related EEG activity in real-life working environments," *Int. J. Psychophysiol.*, vol. 91, no. 1, pp. 3–9, Jan. 2014, doi: 10.1016/j.ijpsycho.2013.10.006.

[14] J. L. Park, P. A. Dudchenko, and D. I. Donaldson, "Navigation in real-world environments: New opportunities afforded by advances in mobile brain imaging," *Frontiers Hum. Neurosci.*, vol. 12, p. 361, Sep. 2018.

[15] J. L. Park, M. M. Fairweather, and D. I. Donaldson, "Making the case for mobile cognition: EEG and sports performance," *Neurosci. Biobehavioral Rev.*, vol. 52, pp. 117–130, May 2015.

[16] T. Castermans, M. Duvinage, M. Petieau, T. Hoellinger, C. D. Saedeleer, K. Seetharaman, A. Bengoetxea, G. Cheron, and T. Dutoit, "Optimizing the performances of a P300-based brain–computer interface in ambulatory conditions," *IEEE J. Emerg. Sel. Topics Circuits Syst.*, vol. 1, no. 4, pp. 566–577, Dec. 2011.

[17] F. Lotte, J. Fujisawa, H. Touyama, R. Ito, M. Hirose, and A. Lécuyer, "Towards ambulatory brain-computer interfaces: A pilot study with P300 signals," in *Proc. Int. Conf. Adv. Comput. Enterntainment Technol.*, 2009, pp. 336–339.

[18] M. M. Fouad, K. M. Amin, N. El-Bendary, and A. E. Hassanien, "Brain Computer Interface: A Review," in *Brain-Computer Interfaces: Current Trends Applysis*, A. E. Hassanien A. T. Azar Eds. Cham, Switzerland: Springer, 2015, pp. 3–30.

[19] S. Debener, F. Minow, R. Emkes, K. Gandras, and M. de Vos, "How about taking a low-cost, small, and wireless EEG for a walk?" *Psychophysiology*, vol. 49, no. 11, pp. 1449–1453, 2012.

[20] K. Gramann, J. T. Gwin, N. Bigdely-Shamlo, D. P. Ferris, and S. Makeig, "Visual evoked responses during standing and walking," *Frontiers Hum. Neurosci.*, vol. 4, p. 202, Oct. 2010, doi: 10.3389/fnhum.2010.00202.

[21] J. T. Gwin, K. Gramann, S. Makeig, and D. P. Ferris, "Electrocortical activity is coupled to gait cycle phase during treadmill walking," *NeuroImage*, vol. 54, no. 2, pp. 1289–1296, Jan. 2011, doi: 10.1016/j.neuroimage.2010.08.066.

[22] A. Gutierrez, R. G. Dreslinski, T. F. Wenisch, T. Mudge, A. Saidi, C. Emmons, and N. Paver, "Full-system analysis and characterization of interactive smartphone applications," in *Proc. IEEE Int. Symp. Workload Characterization (IISWC)*, Nov. 2011, pp. 81–90, doi: 10.1109/IISWC.2011.6114205.

[23] S. Li and S. Mishra, "Optimizing power consumption in multicore smartphones," *J. Parallel Distrib. Comput.*, vol. 95, pp. 124–137, Sep. 2016, doi: 10.1016/j.jpdc.2016.02.004.

[24] G. M. Harari, S. D. Gosling, R. Wang, and A. T. Campbell, "Capturing situational information with smartphones and mobile sensing methods," *Eur. J. Personality*, vol. 29, no. 5, pp. 509–511, Sep. 2015.

[25] B. G. Do Valle, S. S. Cash, and C. G. Sodini, "Wireless behind-the-ear EEG recording device with wireless interface to a mobile device (iPhone/iPod touch)," in *Proc. 36th Annu. Int. Conf. IEEE Eng. Med. Biol. Soc.*, Aug. 2014, pp. 5952–5955, doi: 10.1109/EMBC.2014.6944984.

[26] E. D. McKenzi, "Validation of a smartphone-based EEG among people with epilepsy: A prospective study," *Sci. Rep.*, vol. 7, no. 1, Apr. 2017, Art. no. 45567, doi: 10.1038/srep45567.

[27] A. Campbell, "NeuroPhone: Brain-mobile phone interface using a wireless EEG headset," in *Proc. 2nd ACM SIGCOMM workshop Netw., Syst., Appl. Mobile Handhelds*, 2010, pp. 3–8.

[28] Y.-T. Wang, Y. Wang, and T.-P. Jung, "A cell-phone-based brain-computer interface for communication in daily life," *J. Neural Eng.*, vol. 8, no. 2, 2011, Art. no. 025018.

[29] A. Stopczynski, C. Stahlhut, M. K. Petersen, J. E. Larsen, C. F. Jensen, M. G. Ivanova, T. S. Andersen, and L. K. Hansen, "Smartphones as pocketable labs: Visions for mobile brain imaging and neurofeedback," *Int. J. Psychophysiol.*, vol. 91, no. 1, pp. 54–66, Jan. 2014, doi: 10.1016/j.ijpsycho.2013.08.007.

[30] S. Blum, S. Debener, R. Emkes, N. Volkening, S. Fudickar, and M. G. Bleichner, "EEG recording and online signal processing on android: A multiapp framework for brain-computer interfaces on smartphone," *BioMed Res. Int.*, vol. 2017, pp. 1–12, Mar. 2017.

[31] A. Stopczynski, C. Stahlhut, J. E. Larsen, M. K. Petersen, and L. K. Hansen, "The smartphone brain scanner: A portable real-time neuroimaging system," *PLoS ONE*, vol. 9, no. 2, Feb. 2014, Art. no. e86733.

[32] S. Debener, R. Emkes, M. De Vos, and M. Bleichner, "Unobtrusive ambulatory EEG using a smartphone and flexible printed electrodes around the ear," *Sci. Rep.*, vol. 5, no. 1, Dec. 2015, Art. no. 16743.

[33] G. Sintotskiy and H. Hinrichs, "In-ear-EEG–a portable platform for home monitoring," *J. Med. Eng. Technol.*, vol. 44, no. 1, pp. 26–37, Jan. 2020.

[34] Y.-T. Wang, K.-C. Huang, C.-S. Wei, T.-Y. Huang, L.-W. Ko, C.-T. Lin, C.-K. Cheng, and T.-P. Jung, "Developing an EEG-based on-line closed-loop lapse detection and mitigation system," *Frontiers Neurosci.*, vol. 8, p. 321, Oct. 2014.

[35] G. Li and W.-Y. Chung, "A context-aware EEG headset system for early detection of driver drowsiness," *Sensors*, vol. 15, no. 8, pp. 20873–20893, Aug. 2015.

[36] T.-Y. Wei, D.-W. Chang, Y.-D. Liu, C.-W. Liu, C.-P. Young, S.-F. Liang, and F.-Z. Shaw, "Portable wireless neurofeedback system of EEG alpha rhythm enhances memory," *Biomed. Eng. OnLine*, vol. 16, no. 1, p. 128, Dec. 2017.

[37] A. Sterr, J. K. Ebajemito, K. B. Mikkelsen, M. A. Bonmati-Carrion, N. Santhi, C. della Monica, L. Grainger, G. Atzori, V. Revell, S. Debener, D.-J. Dijk, and M. DeVos, "Sleep EEG derived from behind-the-ear electrodes (cEEGrid) compared to standard polysomnography: A proof of concept study," *Frontiers Hum. Neurosci.*, vol. 12, p. 452, Nov. 2018.

[38] M. R. Nuwer, G. Comi, R. Emerson, A. Fuglsang-Frederiksen, J.-M. Guérit, H. Hinrichs, A. Ikeda, F. Jose C. Luccas, and P. Rappelsburger, "IFCN standards for digital recording of clinical EEG," *Electroencephalogr. Clin. Neurophysiol.*, vol. 106, no. 3, pp. 259–261, Mar. 1998.

[39] M. Piñeyro Salvidegoitia, N. Jacobsen, A. R. Bauer, B. Griffiths, S. Hanslmayr, and S. Debener, "Out and about: Subsequent memory effect captured in a natural outdoor environment with smartphone EEG," *Psychophysiology*, vol. 56, no. 5, May 2019, Art. no. e13331.

[40] A. D. Bateson, H. A. Baseler, K. S. Paulson, F. Ahmed, and A. U. R. Asghar, "Categorisation of Mobile EEG: A Researchers Perspective," *BioMed Res. Int.*, vol. 2017, Oct. 2017, Art no. 5496196, doi: 10.1155/2017/5496196.

[41] Texas-Instruments. (2012). *Low-Noise, 8-Channel, 24-Bit Analog Front-End for Biopotential Measurements ADS1299*. [Online]. Available: http://www.ti.com/product/ADS1299

[42] J. Martin Bland and D. Altman, "Statistical methods for assessing agreement between two methods of clinical measurement," *Lancet*, vol. 327, no. 8476, pp. 307–310, Feb. 1986.

[43] S. Mantha, M. F. Roizen, L. A. Fleisher, R. Thisted, and J. Foss, "Comparing methods of clinical measurement: Reporting standards for bland and altman analysis," *Anesthesia Analgesia*, vol. 90, no. 3, pp. 593–602, Mar. 2000, doi: 10.1097/00000539-200003000-00018.
[44] D. G. Altman and J. M. Bland, "Measurement in medicine: The analysis of method comparison studies," *Statistician*, vol. 32, pp. 307–317, Sep. 1983.
[45] D. Giavarina, "Understanding bland altman analysis," *Biochemia Medica*, vol. 25, no. 2, pp. 141–151, 2015.
[46] J. M. Bland and D. G. Altman, "Measuring agreement in method comparison studies," *Stat. Methods Med. Res.*, vol. 8, no. 2, pp. 135–160, Apr. 1999, doi: 10.1177/096228029900800204.
[47] J. Samaha and B. R. Postle, "The speed of alpha-band oscillations predicts the temporal resolution of visual perception," *Current Biol.*, vol. 25, no. 22, pp. 2985–2990, Nov. 2015, doi: 10.1016/j.cub.2015.10.007.
[48] M. R. Goldstein, M. J. Peterson, J. L. Sanguinetti, G. Tononi, and F. Ferrarelli, "Topographic deficits in alpha-range resting EEG activity and steady state visual evoked responses in schizophrenia," *Schizophrenia Res.*, vol. 168, nos. 1–2, pp. 145–152, 2015. [Online]. Available: http://www.sciencedirect.com/science/article/pii/S0920996415003278
[49] A. Goljahani, C. D'Avanzo, S. Schiff, P. Amodio, P. Bisiacchi, and G. Sparacino, "A novel method for the determination of the EEG individual alpha frequency," *NeuroImage*, vol. 60, no. 1, pp. 774–786, Mar. 2012, doi: 10.1016/j.neuroimage.2011.12.001.
[50] S. Sur and V. Sinha, "Event-related potential: An overview," *Ind. Psychiatry J.*, vol. 18, no. 1, p. 70, 2009.
[51] A. Furdea, S. Halder, D. J. Krusienski, D. Bross, F. Nijboer, N. Birbaumer, and A. Kübler, "An auditory oddball (P300) spelling system for brain-computer interfaces," *Psychophysiology*, vol. 46, no. 3, pp. 617–625, May 2009.
[52] M. Fabiani, G. Gratton, D. Karis, and E. Donchin, "Definition, identification, and reliability of measurement of the P300 component of the event-related brain potential," *Adv. psychophysiol.*, vol. 2, no. 1, p. 78, 1987.
[53] S. Halder, E. M. Hammer, S. C. Kleih, M. Bogdan, W. Rosenstiel, N. Birbaumer, and A. Kübler, "Prediction of auditory and visual P300 brain-computer interface aptitude," *PLoS ONE*, vol. 8, no. 2, Feb. 2013, Art. no. e53513.
[54] NXP-Semiconductors. (2016). *LPC176x/5x User Manual*. [Online]. Available: https://www.nxp.com/docs/en/user-guide/UM10360.pdf
[55] B. W. Kernighan and D. M. Ritchie, *The C Programming Language*, 2nd ed. Englewood Cliffs, NJ, USA: Prentice-Hall, 2006.
[56] NXP-Semiconductors. (2016). *LPC Microcontroller Utilities*. [Online]. Available: https://www.nxp.com/design/microcontrollers-developer-resources/lpc-microcontroller-utilities:LPC-UTILITIES
[57] R. Barry, *FreeRTOS Reference Manual*. Gurugram, Haryana: Real Time Engineers, 2011.
[58] Unity-Technologies. (2015). *Unity Game Engine*. [Online]. Available: https://unity.com/
[59] A. Hejlsberg, S. Wiltamuth, and P. Golde, *C# language Specification*. Reading, MA, USA: Addison-Wesley, 2003.
[60] P. Henderson and R. A. Snowdon, "A tool for structured program development," *Inf. Process.*, vol. 1, pp. 204–207, May 1974.
[61] A. Delorme and S. Makeig, "EEGLAB: An open source toolbox for analysis of single-trial EEG dynamics including independent component analysis," *J. Neurosci. Methods*, vol. 134, p. 9, Feb. 2004, doi: 10.1016/j.jneumeth.2003.10.009.
[62] M. A. Schier, "Changes in EEG alpha power during simulated driving: A demonstration," *Int. J. Psychophysiol.*, vol. 37, no. 2, pp. 155–162, Aug. 2000.
[63] V. Mihajlovic, H. Li, B. Grundlehner, J. Penders, and A. C. Schouten, "Investigating the impact of force and movements on impedance magnitude and EEG," in *Proc. 35th Annu. Int. Conf. IEEE Eng. Med. Biol. Soc. (EMBC)*, Jul. 2013, pp. 1466–1469.
[64] E. S. Kappenman and S. J. Luck, "The effects of electrode impedance on data quality and statistical significance in ERP recordings," *Psychophysiology*, pp. 888–904, Mar. 2010, doi: 10.1111/j.1469-8986.2010.01009.x.
[65] T. C. Ferree, P. Luu, G. S. Russell, and D. M. Tucker, "Scalp electrode impedance, infection risk, and EEG data quality," *Clin. Neurophysiol.*, vol. 112, no. 3, pp. 536–544, 2001, doi: 10.1016/S1388-2457(00)00533-2
[66] O. M. Bazanova and D. Vernon, "Interpreting EEG alpha activity," *Neurosci. Biobehavioral Rev.*, vol. 44, pp. 94–110, Jul. 2014, doi: 10.1016/j.neubiorev.2013.05.007.
[67] S. Haegens, H. Cousijn, G. Wallis, P. J. Harrison, and A. C. Nobre, "Inter- and intra-individual variability in alpha peak frequency," *NeuroImage*, vol. 92, pp. 46–55, May 2014, doi: 10.1016/j.neuroimage.2014.01.049.
[68] C. Bunce, "Correlation, agreement, and Bland–Altman analysis: Statistical analysis of method comparison studies," *Amer. J. Ophthalmology*, vol. 148, no. 1, pp. 4–6, Jul. 2009, doi: 10.1016/j.ajo.2008.09.032.
[69] D. E. J. Linden, "The p300: Where in the brain is it produced and what does it tell us?" *Neuroscientist*, vol. 11, no. 6, pp. 563–576, Dec. 2005, doi: 10.1177/1073858405280524.
[70] R. Zelmann, J. M. Lina, A. Schulze-Bonhage, J. Gotman, and J. Jacobs, "Scalp EEG is not a blur: It can see high frequency oscillations although their generators are small," *Brain Topography*, vol. 27, no. 5, pp. 683–704, Sep. 2014.
[71] E. V. Orekhova, T. A. Stroganova, G. Nygren, M. M. Tsetlin, I. N. Posikera, C. Gillberg, and M. Elam, "Excess of high frequency electroencephalogram oscillations in boys with autism," *Biol. Psychiatry*, vol. 62, no. 9, pp. 1022–1029, Nov. 2007.
[72] R. Friedman, A. Kogan, and Y. Krivolapov, "On power and throughput tradeoffs of WiFi and Bluetooth in smartphones," *IEEE Trans. Mobile Comput.*, vol. 12, no. 7, pp. 1363–1376, Jul. 2013, doi: 10.1109/TMC.2012.117.
[73] S. Pizzamiglio, U. Naeem, H. Abdalla, and D. L. Turner, "Neural correlates of single-and dual-task walking in the real world," *Frontiers Hum. Neurosci.*, vol. 11, p. 460, Sep. 2017, doi: 10.3389/fnhum.2017.00460.
[74] S. Tilley, C. Neale, A. Patuano, and S. Cinderby, "Older People's experiences of mobility and mood in an urban environment: A mixed methods approach using electroencephalography (EEG) and interviews," *Int. J. Environ. Res. Public Health*, vol. 14, no. 2, p. 151, Feb. 2017.
[75] T. C. Bulea, J. Kim, D. L. Damiano, C. J. Stanley, and H.-S. Park, "User-driven control increases cortical activity during treadmill walking: An EEG study," in *Proc. 36th Annu. Int. Conf. IEEE Eng. Med. Biol. Soc.*, Aug. 2014, pp. 2111–2114, doi: 10.1109/embc.2014.6944033.
[76] T. Castermans, M. Duvinage, G. Cheron, and T. Dutoit, "About the cortical origin of the low-delta and high-gamma rhythms observed in EEG signals during treadmill walking," *Neurosci. Lett.*, vol. 561, pp. 166–170, Feb. 2014.
[77] P. De Sanctis, J. S. Butler, B. R. Malcolm, and J. J. Foxe, "Recalibration of inhibitory control systems during walking-related dual-task interference: A mobile brain-body imaging (MOBI) study," *NeuroImage*, vol. 94, pp. 55–64, Jul. 2014.
[78] C. Kranczioch, C. Zich, I. Schierholz, and A. Sterr, "Mobile EEG and its potential to promote the theory and application of imagery-based motor rehabilitation," *Int. J. psychophysiology : Off. J. Int. Org. Psychophysiol.*, vol. 91, no. 1, pp. 5–10, Jan. 2014, doi: 10.1016/j.ijpsycho.2013.10.004.
[79] G. Chéron, M. Duvinage, and C. De Saedeleer, "From spinal central pattern generators to cortical network: Integrated BCI for walking rehabilitation," *Neural Plasticity*, vol. 2012, May 2012, Art. no. 375148, doi: 10.1155/2012/375148.
[80] R. N. Khushaba, C. Wise, S. Kodagoda, J. Louviere, B. E. Kahn, and C. Townsend, "Consumer neuroscience: Assessing the brain response to marketing stimuli using electroencephalogram (EEG) and eye tracking," *Expert Syst. Appl.*, vol. 40, no. 9, pp. 3803–3812, Jul. 2013.
[81] M. Yadava, P. Kumar, R. Saini, P. P. Roy, and D. Prosad Dogra, "Analysis of EEG signals and its application to neuromarketing," *Multimedia Tools Appl.*, vol. 76, no. 18, pp. 19087–19111, Sep. 2017, doi: 10.1007/s11042-017-4580-6.
[82] Y.-K. Fuh and H.-C. Ho, "Highly flexible self-powered sensors based on printed circuit board technology for human motion detection and gesture recognition," *Nanotechnology*, vol. 27, no. 9, Mar. 2016, Art. no. 095401.
[83] B. Meng, W. Tang, X. Zhang, M. Han, W. Liu, and H. Zhang, "Self-powered flexible printed circuit board with integrated triboelectric generator," *Nano Energy*, vol. 2, no. 6, pp. 1101–1106, Nov. 2013, doi: 10.1016/j.nanoen.2013.08.006.
[84] V. Jurcak, D. Tsuzuki, and I. Dan, "10/20, 10/10, and 10/5 systems revisited: Their validity as relative head-surface-based positioning systems," *NeuroImage*, vol. 34, no. 4, pp. 1600–1611, Feb. 2007, doi: 10.1016/j.neuroimage.2006.09.024.
[85] J. Askamp and M. J. van Putten, "Mobile EEG in epilepsy," *Int. J. Psychophysiol.*, vol. 91, no. 1, pp. 5–30, Jan. 2014, doi: 10.1016/j.ijpsycho.2013.09.002.
[86] J. H. Gruzelier, M. Foks, T. Steffert, M. J.-L. Chen, and T. Ros, "Beneficial outcome from EEG-neurofeedback on creative music performance, attention and well-being in school children," *Biol. Psychol.*, vol. 95, pp. 86–95, Jan. 2014, doi: 10.1016/j.biopsycho.2013.04.005.
[87] A. Choo and A. May, "Virtual mindfulness meditation: Virtual reality and electroencephalography for health gamification," in *Proc. Games Media Entertainment (GEM)*, May 2014, pp. 1–3.

[88] B. Murphy, A. Aleni, B. Belaoucha, J. Dyer, and H. Nolan, "Quantifying cognitive aging and performance with at-home gamified mobile EEG," in *Proc. Int. Workshop Pattern Recognit. Neuroimag. (PRNI)*, 2018, pp. 1–4.
[89] L. Szegletes, M. Koles, and B. Forstner, "Socio-cognitive gamification: General framework for educational games," *J. Multimodal User Interface*, vol. 9, no. 4, pp. 395–401, Dec. 2015, doi: 10.1007/s12193-015-0183-6.
[90] T. P. Luu, Y. He, S. Brown, S. Nakagome, and J. L. Contreras-Vidal, "Gait adaptation to visual kinematic perturbations using a real-time closed-loop brain-computer interface to a virtual reality avatar," *J. Neural Eng.*, vol. 13, no. 3, 2016, Art. no. 036006.
[91] M. Wairagkar, I. Zoulias, V. Oguntosin, Y. Hayashi, and S. Nasuto, "Movement intention based brain computer interface for virtual reality and soft robotics rehabilitation using novel autocorrelation analysis of EEG," in *Proc. 6th IEEE Int. Conf. Biomed. Robot. Biomechatron. (BioRob)*, Jun. 2016, p. 685.
[92] M. Näpflin, M. Wildi, and J. Sarnthein, "Test–retest reliability of resting EEG spectra validates a statistical signature of persons," *Clin. Neurophysiol.*, vol. 118, no. 11, pp. 2519–2524, Nov. 2007.
[93] N. A. Badcock, P. Mousikou, Y. Mahajan, P. de Lissa, J. Thie, and G. McArthur, "Validation of the Emotiv EPOC EEG gaming system for measuring research quality auditory ERPs," *PeerJ*, vol. 1, p. e38, Feb. 2013.
[94] G. Jackson, N. Radhu, Y. Sun, K. Tallevi, P. Ritvo, Z. J. Daskalakis, B. Grundlehner, J. Penders, and J. A. Cafazzo, "Comparative evaluation of an ambulatory EEG platform vs. Clinical gold standard," in *Proc. 35th Annu. Int. Conf. Eng. Med. Biol. Soc. (EMBC)*, Jul. 2013, pp. 1222–1225.
[95] A. Omurtag, S. G. A. Baki, G. Chari, R. Q. Cracco, S. Zehtabchi, A. A. Fenton, and A. C. Grant, "Technical and clinical analysis of microEEG: A miniature wireless EEG device designed to record high-quality EEG in the emergency department," *Int. J. Emergency Med.*, vol. 5, no. 1, pp. 1–10, Dec. 2012, doi: 10.1186/1865-1380-5-35.
[96] R. van Dinteren, M. Arns, M. L. A. Jongsma, and R. P. C. Kessels, "P300 development across the lifespan: A systematic review and meta-analysis," *PLoS ONE*, vol. 9, no. 2, Feb. 2014, Art. no. e87347.

ANTHONY D. BATESON was born in Beverley, U.K., in 1970. He received the B.Eng. degree (Hons.) in electronics and communications engineering from the University of Lincolnshire and Humberside, Hull, U.K., in 2001, and the Ph.D. degree in medical sciences from the Hull York Medical School, University of Hull, Hull, in 2019. He is currently a Lecturer with the Department of Engineering, University of Hull. His current research interests include non-invasive brain monitoring (EEG and fNIRS), cognitive load assessment in VR environments, and wound monitoring systems.

AZIZ U. R. ASGHAR received the B.Sc. degree in immunology and pharmacology from the University of Strathclyde, in 1990, and the Ph.D. degree in neuropharmacology from The University of Edinburgh, in 1995.

From 1996 to 2001, he was a Postdoctoral Research Fellow with the Department of Biomedical Sciences, University of Leeds, funded by AstraZeneca and the Wellcome Trust. He was a Lecturer in neuroscience with the University of Leeds, from 2001 to 2003, and a Lecturer in life sciences with the Hull York Medical School, University of Hull, from 2003 to 2019, where he has been a Senior Lecturer in life sciences, since 2019. His research interests include using brain neuroimaging techniques to understand cognition (fMRI, MEG, and EEG), the use of mobile monitors to record brain signals, the utility of virtual and augmented reality systems in the study of cognitive processes, and consumer neuroscience.